

AWARD NUMBER: W81XWH-14-1-0365

TITLE: Macrophage Functions in Early Dissemination and Dormancy of Breast Cancer

PRINCIPAL INVESTIGATOR: Nina Linde

CONTRACTING ORGANIZATION: Ichan School of Medicine at Mount Sinai
New York, NY 10029

REPORT DATE: September 2016

TYPE OF REPORT: Annual

PREPARED FOR: U.S. Army Medical Research and Materiel Command
Fort Detrick, Maryland 21702-5012

DISTRIBUTION STATEMENT: Approved for Public Release;
Distribution Unlimited

The views, opinions and/or findings contained in this report are those of the author(s) and should not be construed as an official Department of the Army position, policy or decision unless so designated by other documentation.

REPORT DOCUMENTATION PAGE

Form Approved
OMB No. 0704-0188

Public reporting burden for this collection of information is estimated to average 1 hour per response, including the time for reviewing instructions, searching existing data sources, gathering and maintaining the data needed, and completing and reviewing this collection of information. Send comments regarding this burden estimate or any other aspect of this collection of information, including suggestions for reducing this burden to Department of Defense, Washington Headquarters Services, Directorate for Information Operations and Reports (0704-0188), 1215 Jefferson Davis Highway, Suite 1204, Arlington, VA 22202-4302. Respondents should be aware that notwithstanding any other provision of law, no person shall be subject to any penalty for failing to comply with a collection of information if it does not display a currently valid OMB control number. **PLEASE DO NOT RETURN YOUR FORM TO THE ABOVE ADDRESS.**

1. REPORT DATE September 2016	2. REPORT TYPE Annual	3. DATES COVERED 1 Sep 2015 - 31 Aug 2016
4. TITLE AND SUBTITLE Macrophage Functions in Early Dissemination and Dormancy of Breast Cancer		5a. CONTRACT NUMBER
		5b. GRANT NUMBER W81XWH-14-1-0365
		5c. PROGRAM ELEMENT NUMBER
6. AUTHOR(S) Nina Linde		5d. PROJECT NUMBER
		5e. TASK NUMBER
		5f. WORK UNIT NUMBER
7. PERFORMING ORGANIZATION NAME(S) AND ADDRESS(ES) Ichan School of Medicine at Mount Sinai New York, NY 10029		8. PERFORMING ORGANIZATION REPORT NUMBER
9. SPONSORING / MONITORING AGENCY NAME(S) AND ADDRESS(ES) U.S. Army Medical Research and Materiel Command Fort Detrick, Maryland 21702-5012		10. SPONSOR/MONITOR'S ACRONYM(S)
		11. SPONSOR/MONITOR'S REPORT NUMBER(S)
12. DISTRIBUTION / AVAILABILITY STATEMENT Approved for Public Release: Distribution Unlimited		
13. SUPPLEMENTARY NOTES		
14. ABSTRACT <p>This research project focuses on the role of macrophages in early dissemination and dormancy. We hypothesized that macrophages are actively recruited by pre-malignant ErbB2 overexpressing cancer cells and that these intra-epithelial macrophages then produce factors that induce an EMT and thereby facilitate early dissemination. We further hypothesized that bone marrow (but not lung) macrophages produce TGFβ2, BMP7 and other factors that instruct DCCs to enter dormancy. In funding year 1 we provided evidence that early ErbB2+ lesions, but not healthy mammary tissue, produced CCL2 in an NFκB dependent manner and thereby recruited resident macrophages inside the duct. Intra-ductal macrophages secreted Wnt1 and thereby induced an EMT in early ErbB2+ cancer cells. Depletion of macrophages - but only before overt advanced tumors appeared - drastically reduced early dissemination and surprisingly the onset of metastasis even after macrophages repopulated the overt tumor tissue. We also proposed that cancer cells that disseminated early play a long-term causal role in metastasis development. In funding year 2 we demonstrated that bone resident macrophages inhibit proliferation of disseminated tumor cells and are responsible for less efficient metastasis formation. When bone resident macrophages are co-injected with breast cancer cells in an experimental metastasis assay in vivo, this significantly reduced lung metastasis formation, demonstrating that resident macrophages can decide over the fate of disseminated tumor cells. We further revealed that bone resident macrophages produce TGFβ2, a factor known to be able to induce dormancy. In contrast, lung resident macrophages produce only low amounts of TGFβ2 and seem to inhibit TGFβ2 production in the lung microenvironment. Overall, these results demonstrate that tissue resident macrophages are highly specific in their function and can decide over the fate of disseminated tumor cells. Overall, the results of this grant have shed light on the mechanism of early dissemination and have revealed a mechanism how macrophages might instruct disseminated tumor cell dormancy in the bone marrow.</p>		

15. SUBJECT TERMS early dissemination, EMT, DCIS, macrophages, tumor microenvironment, metastasis, dormancy, bone metastasis, lung metastasis			
16. SECURITY CLASSIFICATION OF:			17. LIMITATION OF ABSTRACT
a. REPORT	b. ABSTRACT	c. THIS PAGE	Unclassified
Unclassified	Unclassified	Unclassified	
			18. NUMBER OF PAGES
			59
			19a. NAME OF RESPONSIBLE PERSON USAMRMC
			19b. TELEPHONE NUMBER <i>(include area code)</i>

Standard Form 298 (Rev. 8-98)
Prescribed by ANSI Std. Z39.18

TABLE OF CONTENTS

	Page
1. Introduction.....	3
2. Keywords.....	4
3. Abbreviations and Nomenclature.....	4
4. Accomplishments.....	4
5. Impact.....	7
6. Changes / Problems.....	7
7. Products.....	8
8. Participants.....	8
9. References.....	9
10. Appendix 1.....	9

1. INTRODUCTION

Most breast cancer patients die from metastatic disease that are mostly incurable. Metastases can occur years or decades after removal of the primary tumor, suggesting there is a window of opportunity to prevent their outgrowth. Additionally, the field of metastasis research has been challenged by the finding that dissemination does not only occur from late stage invasive tumors but can already occur during early pre-invasive breast cancer stages as revealed by large cohort patient studies [1-4] and studies with spontaneous mouse tumor models [5]. This might lead to an increased heterogeneity of disseminated cancer cells (DCCs) that colonized target organs during different time points of progression and contribute to metastasis. Macrophages were implicated in regulating dissemination (local invasion migration and intravasation) in overt tumors with pathologically defined invasive characteristics [6, 7] and are important for growth of macro-metastases [7, 8], however whether they are involved in early dissemination and the regulation of growth of disseminated tumor cells has never been studied.

In this research project we **hypothesized** that macrophages are actively recruited by pre-malignant ErbB2 overexpressing cancer cells and that these intra-epithelial macrophages then produce factors that induce an EMT and thereby facilitate early dissemination. We further hypothesized that bone marrow (but not lung) macrophages produce TGF β 2, BMP7 and other factors that instruct DCCs to enter dormancy.

In funding year 1 we provided evidence that early ErbB2+ lesions, but not healthy mammary tissue, produced CCL2 in an NF κ B dependent manner and recruited intra-ductal macrophages, that secrete Wnt1 and thereby induce an EMT in the early ErbB2+ cancer cells. Depletion of macrophages before overt advanced tumors appeared drastically reduced early dissemination and surprisingly, the onset of metastasis even after macrophages repopulated the overt tumor tissue. Importantly, humans with DCIS lesions, a very early stage of breast cancer, that contained macrophage+/E-Cadherin^{lo} microenvironments frequently had disseminated cancer cell (DCCs) in the bone marrow. We reveal that resident macrophages can promote early dissemination explaining how early cancer spread might proceed in breast cancer patients. We also propose that eDCCs play a long-term causal role in metastasis development. These results were mostly collected in funding year 1 and are presented in the **manuscript in the appendix**. **In funding year 2 we provide evidence** that lung resident M Φ s induce a proliferation program whereas BM resident M Φ s induce a dormancy program in DCCs. We compared the expression levels of dormancy inducing factors previously described in our lab (TGF β 2, BMP7) and found that BM resident M Φ s produce high levels of TGF β 2 whereas lung resident M Φ s produce low levels and seem to further inhibit TGF β 2 production in the lung microenvironment. We further demonstrated that when bone resident macrophages are co-injected with breast cancer cells in an experimental metastasis assay in vivo, lung metastasis formation was significantly reduced. This demonstrates that resident macrophages can decide over the fate of disseminated tumor cells.

2. KEY WORDS

early dissemination, EMT, DCIS, macrophages, tumor microenvironment, metastasis

3. ABBREVIATIONS AND NOMENCLATURE

We previously referred to cells in very early stage breast cancer lesions as “pre-malignant epithelial cells” (PM-MECs). In the manuscript we changed this nomenclature to “early cancer cells” (eCCs) to address the possibility that there might be a subpopulation of invasive cancer cells within early lesions. Consequently, we refer to “disseminated cancer cells” (DCCs). In the manuscript we also use the synonym Her2 instead of ErbB2. However this is the same protein and mouse model.

EMT – epithelial to mesenchymal transition

DCIS – ductal carcinoma in situ

CC – cancer cell
eCC – early cancer cell
CCC – circulating cancer cell
DCC – disseminated cancer cell

4. ACCOMPLISHMENTS.

Specific Aim 1. To determine the role of MΦs in early dissemination.

Objectives. We will determine which cytokines produced by ErbB2^{hi} / p38^{low} mammary ducts recruit MΦs. We will investigate how intra-epithelial MΦ induce an EMT in ECCs. We will characterize a profile of an early dissemination microenvironment that we will confirm using 3D *in vitro* experiment. We will further confirm the significance of our findings using human tissue microarrays to identify those genes whose expression indicate an early dissemination microenvironment.

Results. All experiments suggested in SA1 have been successfully performed in funding year 1. A manuscript was submitted in October 2015 of which we had provided a copy in the progress report of funding year 1. The manuscript is still under revision and to address reviewer's comments, we performed several additional experiments. We now attach the revised manuscript. The additional experiments that were included in the revised manuscript version are as follows:

- To provide a better overview of the early stages of breast cancer that our study focuses on, we included HE stainings of healthy wild type and pre-malignant mammary glands and invasive tumors (Fig.1A-C).
- We had shown that pre-malignant mammary epithelial cells next to intra-epithelial macrophages show disorganized and reduced E-Cadherin signal. E-Cadherin is an epithelial cell marker and its loss indicates an epithelial to mesenchymal transition. To strengthen our conclusion that intra-epithelial macrophages induce an EMT, we analyzed β -Catenin. We found that early cancer cells adjacent to intra-epithelial macrophages contain (Fig.2E-G), strengthening our conclusion that intra-epithelial macrophages induce an EMT. We had performed a mass cytometry (CyTOF) analysis of mammary gland macrophages. We now expanded this analysis, including more animals in the experiment (Fig.5). Additionally, the CyTOF analysis was complemented by *in situ* stainings of CD206 in wild type and pre-malignant mammary glands as well as invasive tumors (Fig.5K-N).
- We had identified that CCL2 produced by HER2⁺ early cancer cells was responsible to attract macrophages into pre-malignant ducts. We now confirmed those findings by performing stainings revealing the presence of CCL2 next to HER2⁺ early cancer cells and CCR2⁺ macrophages (Fig.6C). Additionally, we had blocked the receptor for CCL2, CCR2, systemically. To address whether macrophages recruited into the duct were circulation derived or resident tissue derived, we now also blocked CCR2 locally by injecting the inhibitor into the mammary fat pad on one side and treated the contra-lateral mammary gland with vehicle control. We found that those glands injected with the CCR2 inhibitor contained less ducts with intra-epithelial macrophages compared to the contra-lateral control treated glands (Fig.6N,O). If CCR2 inhibition was affecting circulating macrophage precursors, then local injection of the CCR2 inhibitor should not affect macrophage localization. The results therefor indicate that intra-epithelial macrophages are derived from resident tissue macrophages.

Specific Aim 2: To determine how target organ-specific MΦ dictate DCC fate.

Objectives. To determine how lung resident MΦs induce a proliferation program and how BM resident MΦs induce a dormancy program in DCCs. We will compare expression profiles of lung and BM resident MΦs and compare expression levels of dormancy inducing factors previously described in our lab (i.e. TGF β 2, BMP7). We will validate identified factors responsible for the induction of a dormancy program *in vitro* and *in vivo*.

Task 1: Direct effect of lung and BM and lung MΦs on tumor cell proliferation

We completed *SA2.1a* and confirmed the adverse effect of lung and BM MΦs on tumor cell proliferation *in vitro* (Fig.2.1). We included a 2D proliferation assay and confirmed that CM from lungs stimulates 4T1 cell proliferation in 2D but this is reversed when macrophages are depleted. In contrast, CM from BM inhibits proliferation but only when BM contains macrophages. This method will provide a good and simple assay to screen for the effect of macrophage derived factors on dormancy (see SA2.3). Using a mammosphere assay, we could confirm the specific effect of lung and BM CM from macrophage depleted or control treated animals (Fig.2.1B-F). All these experiments have been repeated 3 times with high reproducibility and are thus sufficient for publication.

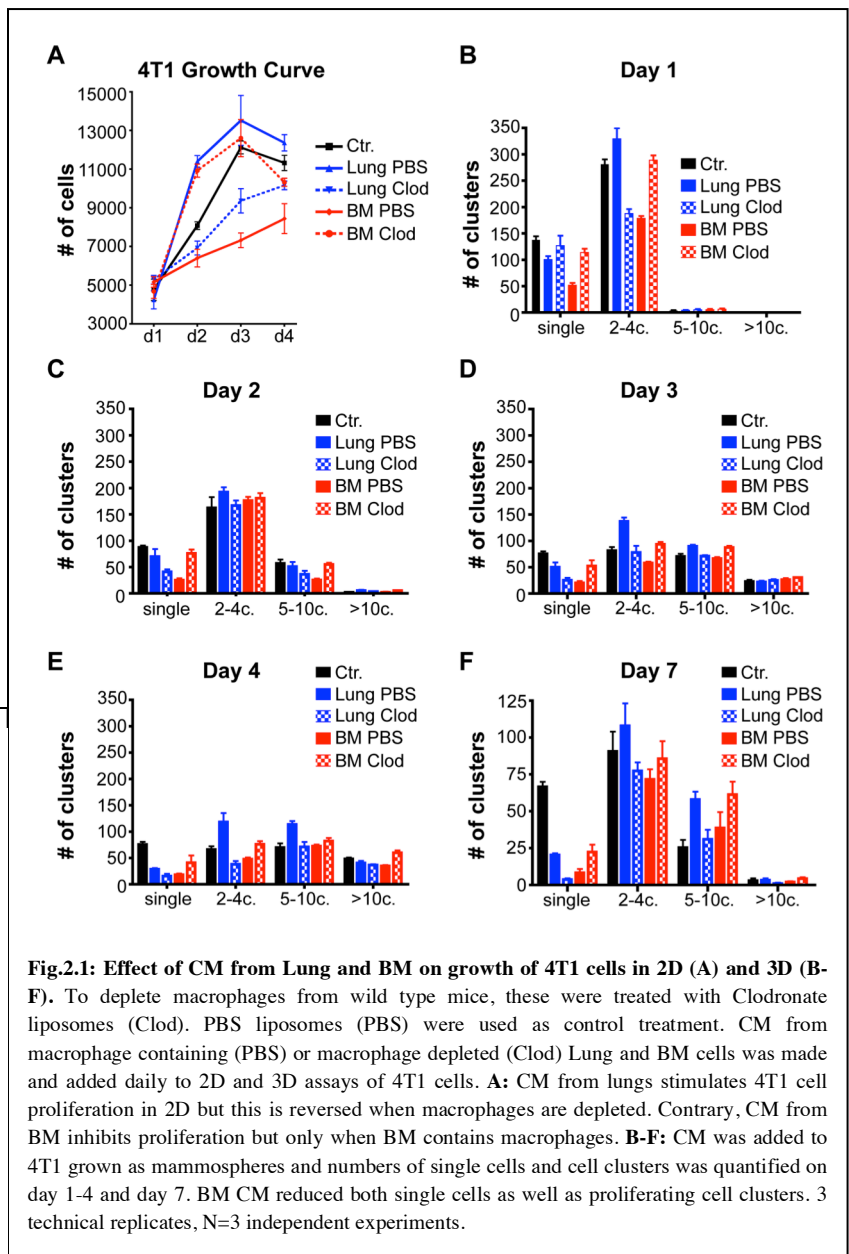


Fig.2.1: Effect of CM from Lung and BM on growth of 4T1 cells in 2D (A) and 3D (B-F). To deplete macrophages from wild type mice, these were treated with Clodronate liposomes (Clod). PBS liposomes (PBS) were used as control treatment. CM from macrophage containing (PBS) or macrophage depleted (Clod) Lung and BM cells was made and added daily to 2D and 3D assays of 4T1 cells. **A:** CM from lungs stimulates 4T1 cell proliferation in 2D but this is reversed when macrophages are depleted. Contrary, CM from BM inhibits proliferation but only when BM contains macrophages. **B-F:** CM was added to 4T1 grown as mammospheres and numbers of single cells and cell clusters was quantified on day 1-4 and day 7. BM CM reduced both single cells as well as proliferating cell clusters. 3 technical replicates, N=3 independent experiments.

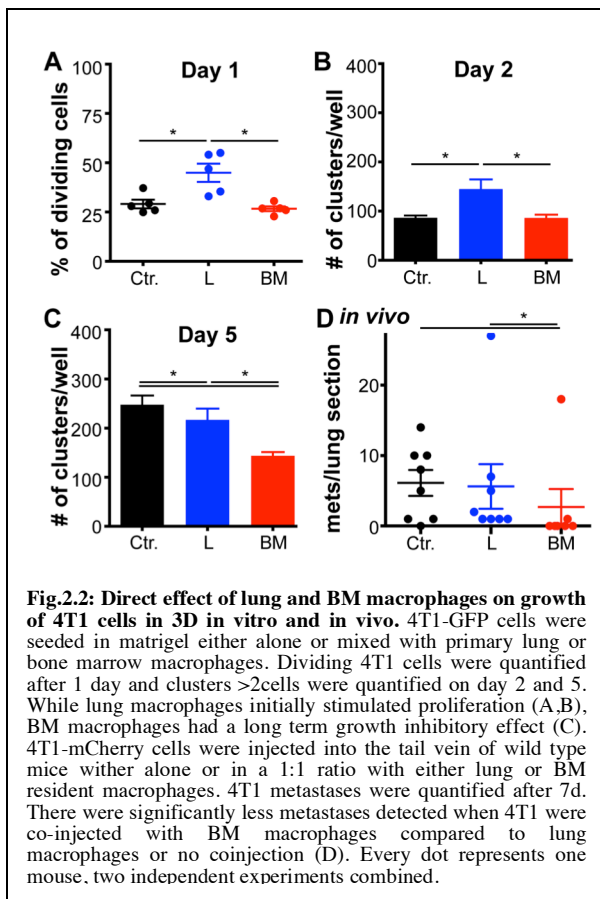


Fig.2.2: Direct effect of lung and BM macrophages on growth of 4T1 cells in 3D in vitro and in vivo. 4T1-GFP cells were seeded in matrigel either alone or mixed with primary lung or bone marrow macrophages. Dividing 4T1 cells were quantified after 1 day and clusters >2cells were quantified on day 2 and 5. While lung macrophages initially stimulated proliferation (A,B), BM macrophages had a long term growth inhibitory effect (C). 4T1-mCherry cells were injected into the tail vein of wild type mice with alone or in a 1:1 ratio with either lung or BM resident macrophages. 4T1 metastases were quantified after 7d. There were significantly less metastases detected when 4T1 were co-injected with BM macrophages compared to lung macrophages or no coinjection (D). Every dot represents one mouse, two independent experiments combined.

As further proposed, we tested the direct effect of lung and BM resident MΦs on cancer cell proliferation by performing a direct 3D co-culture (Fig.2.2A-C). We found that while lung macrophages initially stimulated proliferation (Fig.2.2A,B), BM macrophages had a long term growth inhibitory effect, resulting in less 4T1 cancer cell cluster formation (Fig.2.2C).

We further completed *SA2.1b* and We then confirmed these findings in an experimental metastasis vivo and co-injected 4T1-mCherry cancer cells with either lung or BM

resident MΦs. The addition of BM MΦs significantly reduced metastasis formation compared to co-injection with lung MΦs or injection of 4T1 cancer cells alone (Fig.2.2D).

Task 2: Expression of dormancy-inducing factors in lung and BM MΦs.

As proposed in SA2.2a, we determined TGFβ2 produced by resident macrophages from either lung or BM (Fig.2.3). We found that TGFβ2 levels were higher in total BM and primary BM MΦs CM compared to total lung and lung MΦ CM. Additionally, when MΦs had been removed from the organ cell suspensions by FACS sorting (Fig.2.3 “all cells but macs”), this significantly increased TGFβ2 levels in lung suspension and significantly reduced TGFβ2 levels in BM suspension. Similarly, TGFβ2 levels increased in lung suspension but decreased in BM suspensions when macrophages were depleted in vivo using clodronate liposomes. This provided a quantitative confirmation of our preliminary data analyzing TGFβ2 levels by Western Blot (see initial grant application. As further proposed in SA2.2a, we also analyzed BMP7 levels by ELISA but did not find significant differences in BMP7 secretion by BM or lung MΦs (data not shown).

Previous work from our lab has shown that high TGFβ2 induce dormancy in disseminated cancer cells [9]. We could confirm that 4T1 cancer cells show reduced proliferation in conditions under which TGFβ2 levels are high. Additionally we could now show that bone resident macrophages are the direct source of TGFβ2, indicating that bone macrophages induce dormancy in disseminated cancer cell reaching the bone microenvironment. Lung macrophages do not express high levels of TGFβ2 and seem to further inhibit the production of TGFβ2 in the lung microenvironment.

As proposed in SA2.2b we are currently pursuing a non-targeted approach to identify unknown MΦ-derived factors that mediate induction and exit from dormancy. To this end, we are analyzing conditioned medium as it was used for the TGFβ2 ELISA by mass spectrometry to detect proteins that are a) secreted by BM MΦs and induce cancer cell dormancy or b) secreted by L MΦs and allow escape from dormancy. The results of the mass spectrometry analysis are not available yet. This effort will be continued in the lab of the PI's mentor Dr. Aguirre-Ghiso.

Task 3: Validation of MΦ-derived dormancy inducing factors.

This effort was proposed for funding year 3 in SA2.3.

Training opportunities. The training opportunities according to the statement of work were met; these training opportunities were: sorting of mammary gland macrophages; performing RealTime PCRs, performing 2D and 3D in vitro cultures, use combinatory pharmacologic inhibitors, isolate and cultivate BM and lung MΦs, perform mammosphere cultures, perform tail vein injections, perform cryosections. Additionally, meetings with the Co-mentor Dr. Merad and Dr. Aguirre-Ghiso were held as well as with the mentoring committee to discuss progress of the project.

Dissemination of results to the community. The work presented here is part of a research manuscript that is under revision in Nature Communications. Additionally, the results have been presented in several conferences (see Product section).

Plans for the next funding period. The PI has accepted a lab head position with Merck KGaA in Germany and will therefore not be able to continue the work in the next funding period. The PI's mentor will most likely continue the project and apply for additional funding sources to do so.

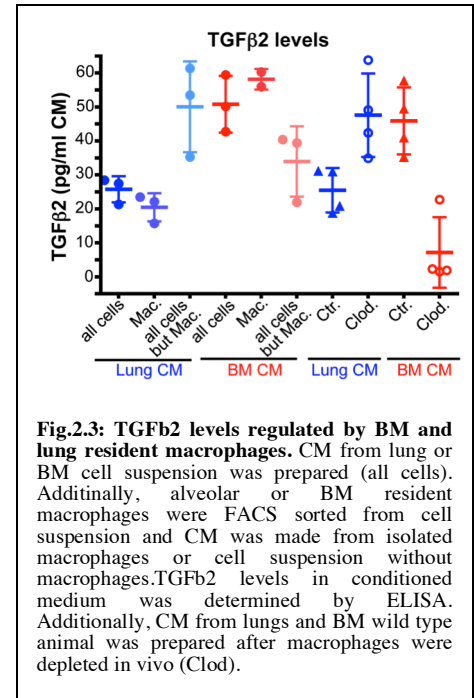


Fig.2.3: TGFβ2 levels regulated by BM and lung resident macrophages. CM from lung or BM cell suspension was prepared (all cells). Additionally, alveolar or BM resident macrophages were FACS sorted from cell suspension and CM was made from isolated macrophages or cell suspension without macrophages. TGFβ2 levels in conditioned medium was determined by ELISA. Additionally, CM from lungs and BM wild type animal was prepared after macrophages were depleted in vivo (Clod).

5. IMPACT

Approximately 90% of breast cancer patients die from commonly incurable metastases. Metastases can occur years or decades after removal of the primary tumor, suggesting there is a window of opportunity to prevent their outgrowth. Additionally, recent clinical data demonstrating that dissemination can occur much earlier than assumed and that patients carrying pathologically defined pre-invasive breast cancer lesions (e.g. ductal carcinoma in situ, DCIS) can carry dormant DCCs. This has caused great confusion on how to treat women with early stage breast cancer such as DCIS. A recent study published in JAMA Oncology [10] adds to this confusion as it shows that while breast cancer deaths from DCIS are rare, 50% of those cases occur in the absence of an invasive breast cancer recurrence and that the choice of therapy did not affect survival. This indicates that albeit at early frequency, a subpopulation of women with DCIS carry early disseminated cancer cells that can have deadly consequences. We therefore need better tools to identify those DCIS patients at high risk of developing late metastatic relapses without overtreating the majority of women who have harmless variants of DCIS. Our mechanistic work on early dissemination that we were able to carry out with the support of this DoD breast cancer award has led us to the notion that those DCIS lesions carrying an E-Cadherin low/macrophage high signature might be indicative of the presence of disseminated disease.

6. CHANGES/PROBLEMS

No major changes or problems.

7. PRODUCTS

Manuscripts:

„Macrophages orchestrate early dissemination of HER2+ cancer cells.“ Nina Linde, Arthur Mortha, Eduardo Farias, Maria Soledad Sosa, Kathryn Harper, Ethan Tardio, Miriam Merad, and Julio A. Aguirre-Ghiso. – *Manuscript under revision in Nature Communications.*

„The relationship between dormant cancer cells and their microenvironment.“ Nina Linde^{*#}, Georg Fluegen^{*#}, and Julio A. Aguirre-Ghiso[#]. – *Invited Book Chapter for **Advances in Cancer Research**. In press. *Both authors contributed equally. #Corresponding author.*

Oral Presentations:

„Macrophages orchestrate early metastatic dissemination of pre-malignant ErbB2+ mammary epithelial cells“
Cancer Biology Retreat, Mount Sinai, New York, NY, December 2014

Awards:

Icahn School of Medicine at Mount Sinai Postdoctoral Recognition Award, New York, December 2014
AACR Scholar in Training Award 2016

Poster presentations:

„Macrophages orchestrate early metastatic dissemination of pre-malignant ErbB2+ mammary epithelial cells“
Annual Meeting of the American Society of Cell Biology, Philadelphia, PA, December 2014

„Macrophages orchestrate early metastatic dissemination of pre-malignant ErbB2+ mammary epithelial cells“
Cancer Cell Symposium on Cancer Inflammation, Sitges, Spain, June 2015

„Macrophages orchestrate early dissemination of HER2+ cancer cells“ Annual Meeting American Association
of Cancer Research, New Orleans, LA, April 2016

„Macrophages orchestrate early dissemination of HER2+ cancer cells“ American Association of Cancer
Research Tumor Metastasis Meeting, Austin, TX, November 2015

8. PARTICIPANTS

no change

9. LITERATURE

1. Braun, S., et al., *A pooled analysis of bone marrow micrometastasis in breast cancer*. N Engl J Med, 2005. **353**(8): p. 793-802.
2. Banys, M., et al., *Hematogenous and lymphatic tumor cell dissemination may be detected in patients diagnosed with ductal carcinoma in situ of the breast*. Breast Cancer Res Treat, 2012. **131**(3): p. 801-8.
3. Schardt, J.A., et al., *Genomic analysis of single cytokeratin-positive cells from bone marrow reveals early mutational events in breast cancer*. Cancer Cell, 2005. **8**(3): p. 227-39.
4. Sanger, N., et al., *Disseminated tumor cells in the bone marrow of patients with ductal carcinoma in situ*. Int J Cancer, 2011. **129**(10): p. 2522-6.
5. Husemann, Y., et al., *Systemic spread is an early step in breast cancer*. Cancer Cell, 2008. **13**(1): p. 58-68.
6. Lin, E.Y., et al., *Colony-stimulating factor 1 promotes progression of mammary tumors to malignancy*. J Exp Med, 2001. **193**(6): p. 727-40.
7. Qian, B., et al., *A distinct macrophage population mediates metastatic breast cancer cell extravasation, establishment and growth*. PLoS One, 2009. **4**(8): p. e6562.
8. Qian, B.Z. and J.W. Pollard, *Macrophage diversity enhances tumor progression and metastasis*. Cell, 2010. **141**(1): p. 39-51.
9. Bragado, P., et al., *TGF-beta2 dictates disseminated tumour cell fate in target organs through TGF-beta-RIII and p38alpha/beta signalling*. Nat Cell Biol, 2013. **15**(11): p. 1351-61.
10. Narod, S.A., et al., *Breast Cancer Mortality After a Diagnosis of Ductal Carcinoma In Situ*. JAMA Oncol, 2015.

10. APPENDIX: Manuscript on the following pages

1 **Macrophages orchestrate early dissemination and**
2 **metastasis of HER2+ cancer cells.**

3

4 Nina Linde¹, Arthur Mortha², Adeeb Rahman³, Eduardo Farias¹, Maria Soledad Sosa¹,
5 Kathryn Harper¹, Ethan Tardio¹, Miriam Merad^{2,3}, and Julio A. Aguirre-Ghiso^{1,4}.

6

7 ¹Division of Hematology and Oncology, Department of Medicine, Department of
8 Otolaryngology, Tisch Cancer Institute, Black Family Stem Cell Institute, Icahn School
9 of Medicine at Mount Sinai, New York, NY, USA.

10 ²Department of Oncological Sciences, The Immunology Institute, Tisch Cancer Institute,
11 Icahn School of Medicine at Mount Sinai, New York, NY, USA

12 ³Human Immune Monitoring Core, Icahn School of Medicine at Mount Sinai, New York,
13 NY, USA

14

15 ⁴Correspondence: julio.aguirre-ghiso@mssm.edu

16

17

18

19 **Abstract**

20 Cancer cell dissemination can occur during very early stages of breast cancer but the
21 mechanisms controlling this process and how they contribute to metastasis are unclear.
22 Here we show that MMTV-HER2 early cancer lesions contain an invasive subpopulation
23 of HER2+/E-cadherin-lo cancer cells that depend on macrophages for dissemination.
24 Macrophages produced Wnt-1 and induced loss of E-cadherin and dissemination of
25 early HER2+ cancer cells. Depletion of macrophages before overt tumor detection
26 drastically reduced early dissemination and diminished the onset of metastasis even
27 when macrophage depletion was stopped when tumors became invasive. Resident
28 CCR2+/CD206+/VCAM-/Tie2+ macrophages were attracted into early lesions by CCL2
29 produced by early HER2+ cancer cells in an NFkB-dependent manner. Intra-epithelial
30 macrophages and loss of E-cadherin junctions was also found in human DCIS, but not
31 normal breast tissue. We reveal a previously unrecognized mechanism by which
32 macrophages play a causal role in early dissemination impacting long-term metastasis
33 development.

34

35

36 Introduction

37 The paradigm of cancer metastasis states that dissemination and metastasis
38 occur when advanced aggressive tumors acquire invasive mechanisms. The finding that
39 dissemination does not only occur from late stage invasive tumors has challenged this
40 model ¹. Large cohort patient studies ²⁻⁵ and studies with spontaneous mouse tumor
41 models ⁶ showed that dissemination also occurs during early stages of cancer when
42 lesions are diagnosed by light microscopy as pre-malignant or pre-invasive. In addition,
43 cancer of unknown primary is a relatively frequent event in solid cancers where
44 metastases develop without the presence of an obvious primary tumor mass that
45 evolved to become invasive ⁷.

46 The “early dissemination” definition was refined by Husemann et al. ⁶ when they
47 showed that early disseminated cancer cells (DCCs) originate at times when lesions are
48 only defined *in situ* by light microscopy (e.g. ductal carcinoma in situ (DCIS) in humans
49 and mammary intraepithelial neoplasia in mice) but dissemination occurs and early
50 DCCs show few genetic aberrations. In the MMTV-HER2 model, early DCCs are able to
51 form lung metastases in the absence of invasive carcinoma ⁶. This argues that in these
52 models early DCCs are endowed with latent metastasis initiating capacity. Similarly,
53 women treated for DCIS can develop metastases without ever developing any
54 subsequent local invasive breast cancer ⁸⁻¹². This might indicate that, albeit at low
55 frequency, early DCCs can unpredictably form metastases in patients. Early
56 dissemination is not a rarity of breast cancer models (MMTV-HER2 and -PyMT models
57 ⁶, as it also occurs in spontaneous mouse models of melanoma ¹³ and pancreatic
58 cancer ¹⁴.

59 While in K-Ras-driven pancreatic cancer an EMT has been linked to early
60 dissemination ¹⁴, its contribution to metastasis is unknown. Further, it remains poorly
61 understood how dissemination occurs during pre-invasive stages of breast cancer when
62 the epithelium-to-stroma barrier is intact. Early DCCs displayed only few genetic
63 alterations ^{4,6}, indicating that early dissemination might be driven by epigenetic and
64 micro-environmental mechanisms that turn on programs of epithelial cell motility ^{15,16}. In
65 fact, invasion of epithelial cells occurs physiologically during development.

66 The mammary epithelium forms postnatally during adolescence in a process
67 called branching morphogenesis where rapidly dividing epithelial cells elongate the
68 terminal end bud into the fat pad and bifurcate into the ductal tree. Macrophages are
69 key regulators of branching morphogenesis during mammary gland development ^{17,18},
70 arguing that normal mammary epithelial cells cooperate with these innate immune cells
71 for invasive processes. These data led to the discovery of macrophages as powerful
72 drivers of intravasation from invasive breast cancer tumors *via* the establishment of
73 tumor microenvironments of metastasis ¹⁹. This follows a streaming process where
74 breast cancer cells recruit macrophages *via* production of colony stimulating factor 1
75 (CSF1) and then cancer cell motility is stimulated *via* macrophage-derived EGF ²⁰.
76 Additionally, macrophages can induce an epithelial to mesenchymal transition (EMT) in
77 malignant cells ^{21,22}. However, the role of macrophages in early spread of cancer
78 remained unexplored.

79 Here we show that the branching morphogenesis program is altered by the
80 HER2 oncogene early in cancer development. Mammary tissue macrophages are
81 recruited by HER2+ early cancer cells from the stroma into the epithelial layer of lesions

82 defined as mammary intraepithelial neoplasia in mice (similar to DCIS in humans) ²³.
83 This process depends on HER2-NFκB-mediated induction of CCL2. CCR2+ intra-
84 epithelial macrophages respond to CCL2, produce Wnt-1 and disrupt the myo-epithelial
85 layer locally by downregulating E-cadherin junctions in a subpopulation of HER2+
86 cancer cells. Before tumors form, these events result in early dissemination
87 microenvironments that propel active intravasation and dissemination to the lung that
88 was efficiently blocked by macrophage depletion. Transient depletion of macrophages
89 in mice before the formation of invasive tumors reduced lung metastatic burden.
90 Importantly, this was the case when macrophage depletion had been stopped with
91 formation of invasive tumors and mice were followed until they carried large overt
92 invasive tumors. Our results suggest a previously unrecognized role for HER2-mediated
93 recruitment of macrophages to favor dissemination of HER2+ tumor cells much earlier
94 than growth is induced by the oncogene. Our work also reveals a role for early DCCs in
95 supporting late metastasis development.

96

97 **RESULTS**

98 **MACROPHAGES INFILTRATE THE EPITHELIAL COMPARTMENT OF EARLY HER2+ MAMMARY** 99 **CANCER LESIONS.**

100 We asked whether the HER2 oncogene might recruit macrophages to
101 orchestrate early dissemination. We used MMTV-HER2 mice as a murine model of
102 breast cancer since these show slow progression from early lesions such as
103 hyperplasia and mammary intra-epithelial neoplasia (**Fig.1A,B**), the latter a similar
104 lesion to DCIS ²³, to invasive tumors (**Fig.1C**). We stained MMTV-HER2 mammary

105 gland sections for the murine macrophage marker F4/80 before we could detect any
106 signs of invasive tumor masses in serial sections of mammary tissue or even enhanced
107 proliferation in HER2+ early lesions²⁴. Macrophages were located to the stroma outside
108 of mammary ducts in healthy FVB wild type animals (**Fig.1D**). This was also true in
109 young 14wk old MMTV-HER2 mice (**Fig.1E**). However, when MMTV-HER2 mice
110 progressed over time but still showed no signs of tumor masses or enhanced
111 proliferation²⁴, macrophages were often localized inside the luminal epithelial layer of
112 early lesions as demonstrated by co-staining of F4/80 and cytokeratin 8/18 (**Fig. 1F**).
113 We hypothesized that as macrophages enter the early lesions, they might disrupt the
114 architecture of the duct. Close inspection of sections co-stained for smooth muscle actin
115 and F4/80 showed that the myoepithelial cell layer was frequently disrupted at sites
116 where macrophages were in immediate contact with the duct (**Fig. 1G-I**). Quantification
117 of the abundance of intra-epithelial macrophages confirmed that the incidence of ducts
118 with intra-epithelial macrophages correlated with HER2 upregulation and disease
119 progression (**Fig. 1J**).

120

121 **MACROPHAGES DISMANTLE E-CADHERIN JUNCTIONS IN EARLY HER2+ CANCER CELLS.**

122 We hypothesized that HER2 might aberrantly activate a mechanism of invasion
123 and motility involving macrophages in early lesions. We found that intra-epithelial
124 macrophages were associated with a strong local downregulation of E-cadherin
125 junctions *in vivo* in early lesion cells located directly adjacent to macrophages (1-2 cell
126 diameter away) (**Fig.2A-C**). This was paralleled by a general downregulation of E-
127 Cadherin mRNA in early lesions compared to wild type glands (**Fig.2D**). Additionally, β -

128 Catenin levels were increased in early lesions containing intra-epithelial macrophages
129 as measured by dual color IHC (**Fig.2E-G**). A loss of E-Cadherin and translocation of β -
130 Catenin to the nucleus could also be induced *in vitro* when Raw264.7 macrophages
131 were added to Comma-1D healthy mammary epithelial cell monolayers used as a
132 readout for epithelial junction formation (**Fig.2H-J**). The loss of E-cadherin junctions in
133 epithelial cells adjacent to macrophages suggested that macrophages might produce
134 cues that stimulate a loss of E-cadherin junctions as observed during the epithelium to
135 mesenchyme transition (EMT). Macrophages can produce Wnt ligands²⁵⁻²⁷ which are
136 potent inducers of an EMT. We therefore tested the response of Raw264.7
137 macrophages or primary mammary tissue macrophages isolated from early lesions to
138 conditioned media from healthy epithelial cells or from HER2+ early cancer cells. Only
139 conditioned media derived from HER2+ cells induced an upregulation of Wnt-1 (**Fig.2K,**
140 **L**); no changes were detected for Wnt-3, Wnt5a and Wnt7 (data not shown). The loss of
141 E-Cadherin junctions in Comma-1D cells induced by Raw264.7 macrophages was
142 reversed by addition of DKK1, an inhibitor of canonical Wnt signaling, to the co-cultures
143 (**Fig.2M-P**). We conclude that downregulation of E-cadherin mRNA and junctions and β -
144 catenin upregulation and nuclear translocation in early lesion cells results from HER2-
145 dependent recruitment of Wnt-1 secreting macrophages into the early lesions.

146 **MACROPHAGE DEPLETION PREVENTS AN E-CADHERIN AND β -CATENIN JUNCTION DISASSEMBLY**
147 **AND EARLY DISSEMINATION.**

148 Our data indicated that HER2 leads to macrophage mobilization into early lesions
149 where they induce an EMT in early cancer cells. We next tested whether this process
150 leads to early dissemination. CSF1R is expressed by most tissue resident macrophages

151 and is required for macrophages survival in tissues ²⁸. Thus, we injected MMTV-HER2
152 mice during early lesions with a blocking antibody to Csf-1 receptor (CSF1R) to
153 eliminate macrophages from early lesions and then quantified circulating and
154 disseminated early cancer cells in blood and target organs respectively (**Fig.3A**).
155 CSF1R blockade led to efficient depletion of tissue resident CD11b⁺/F4/80⁺/Gr1⁺
156 macrophages (**Supplementary Fig.1A**). Immunofluorescence staining for F4/80 in
157 HER2⁺ early lesions confirmed a significant reduction in the number of intra-epithelial
158 macrophages when CSF1R was blocked (**Supplementary Fig.1B**). We confirmed that
159 at the end of the experiment, no tumor masses had formed, by inspecting whole mount
160 stainings of mammary glands (**Supplementary Fig.1D,E**) and HE staining of serially
161 sectioned mammary tissue (**Fig.3B,C**). Macrophage depletion was accompanied by a
162 significant reduction in the number of hyperplastic ducts (**Supplementary Fig.1C**) and a
163 tissue wide upregulation of E-Cadherin mRNA (**Fig.3D**) and E-Cadherin-based junctions
164 (**Fig.3E-G**). We conclude that macrophages contribute to the loss of E-cadherin mRNA
165 and junctions and disrupted mammary tissue architecture in early lesions.

166 The above changes correlated with the finding that CSF1R blockade significantly
167 reduced the numbers of early circulating cancer cells (**Fig.3H**). Accordingly, CSF1R
168 blockade also reduced early disseminated cancer cell (DCC) burden in target organs as
169 measured by the detection of the transgene surface HER2 expressing early DCCs in
170 the lungs (**Fig.3I-K**). We conclude that macrophages play a critical role in the ability of
171 early cancer cells to acquire an invasive and disseminating phenotype. As indicated
172 previously, these events of dissemination take place during a stage where no invasive

173 tumors are detectable and early lesions show similar proliferative capacity than normal
174 resting mammary epithelium²⁴.

175

176 **HER2-RECRUITED MACROPHAGES CONTROL EARLY DISSEMINATION AND CONTRIBUTE TO**
177 **METACHRONOUS METASTASIS FORMATION.**

178 We next tested whether macrophage-regulated early dissemination contributed
179 to metastasis formation. To this end we blocked CSF1R only during early asymptomatic
180 stages of cancer, starting at age week 18, and stopped as soon as tumors became
181 palpable (size <3mm in diameter). We then waited until tumors reached 1 cm in
182 diameter (4-6 weeks later) and quantified solitary DCCs and metastatic lesions in lungs
183 (**Fig.4A**). We found that the time to tumor detection was slightly delayed when
184 macrophages were depleted during asymptomatic pre-malignant stages (**Fig.4B**).
185 However, once palpable tumors had formed, the progression to overt tumors was not
186 affected (**Fig.4C**). Additionally, overt tumors showed no difference in macrophage
187 content (**Fig.4D-F**) and vascularization (**Fig.4G-J**) at the end of the experiment between
188 control and anti-CSF1R treated mice. This suggests that there is no impact on overt
189 tumor growth in late tumors when macrophages were depleted during early stages.
190 Additionally, flow analysis of lungs revealed that neither alveolar macrophage nor
191 CD11b+/Gr1+ monocyte content was significantly affected (**Supplementary Fig.2A-E**)
192 by the same treatment arguing against a systemic loss of all macrophages. However,
193 CSF1R blockade during early stages significantly decreased solitary DCC burden in
194 lungs (**Fig.4K**). CSF1R blockade during early stages also caused a statistically
195 significant decrease in the number of metachronous metastases per mouse (**Fig.4M**),

196 which were defined as the number of metastatic lesions bigger than three cells (**Fig.4L**).
197 This inhibitory effect of DCC burden and metastasis was detected even after
198 macrophage depletion had been stopped in average for one month and animals had
199 carried fast-growing tumors. That the number of solitary DCCs, likely a mixture of DCCs
200 accumulated since the early stages was reduced by CSF1R blockade suggests that the
201 reduced influx of DCCs to lungs during early stages was not replaced by DCCs arriving
202 during the time of tumor detection to euthanasia when tumors were large. We conclude
203 that HER2+ early cancer cells recruit macrophages and that these play a seminal role in
204 early dissemination, allowing for the early DCCs to reach target organs and form
205 metastasis.

206

207 **HETEROGENEITY OF MYELOID CELLS IN EARLY MIN LESIONS.**

208 Our data suggests that macrophages play an active role in favoring early
209 dissemination and that early DCCs contribute to metachronous metastasis formation.
210 Remarkably, this occurs during early cancer stages in the absence of highly proliferative
211 tumor masses when the mammary tree mostly resembles that of a healthy gland. We
212 hypothesized that dissemination might be facilitated by tissue resident macrophages
213 involved in programs of branching morphogenesis during mammary gland development
214 ^{17,29}. We therefore compared the phenotype of macrophages present in wild type and
215 early lesion mammary glands. Mammary glands derived from FVB wild type mice and
216 MMTV-HER2 early lesion at 14 and 22 weeks were analyzed using CyTOF with a panel
217 of 17 hematopoietic cell markers and IdU as a proliferation marker (**Supplementary**
218 **Fig.3A**). Myelo-monocytic cells were identified as CD45+CD11b+F4/80+ cells lacking

219 lymphoid and granulocytic markers (**Supplementary Fig.3B**). viSNE plots ³⁰ of myelo-
220 monocytic cells (**Fig.5A**) showed that myelomonocytic numbers and patterns were
221 similar between wild type glands and early lesions. viSNE analysis further revealed
222 three putative populations, one of which could be identified as monocyte based on its
223 high Ly6C levels (**Fig.5B**) and did not differ in numbers between these samples
224 (**Fig.5D**). The remaining LY6C- macrophages could be distinguished into two
225 populations according to the expression of CD206 (**Fig.5C**). The pre-dominant
226 macrophage subtype present in both wild type glands and early lesions was CD206^{hi}
227 (**Fig.5E,F**). CD206-hi macrophages were also Tie2^{hi}, CD11b^{hi} and VCAM-lo and did not
228 show any signs of proliferation based on IdU incorporation (**Fig.5I,J; Supplementary**
229 **Fig.3C,D**). This matches previous findings ³¹ that wild type resident mammary glands
230 contained M2 polarized CD11b^{hi}, CD206^{hi} and Tie2^{hi} macrophages termed mammary
231 tissue macrophages (MTMs) whereas tumor-associated macrophages prevalent in
232 invasive MMTV-PyMT tumors were CD11b^{int}, CD206^{lo}, Tie2^{lo} and VCAM^{hi}. We found
233 that these CD206^{lo} TAMs were a minority in wild type glands or early lesions but indeed
234 constituted the majority of myelomonocytic cells in overt invasive MMTV-HER2 tumors
235 (**Fig.5G,H**). Since our global CyTOF analysis showed that the predominant macrophage
236 population in HER2+ early lesions resembled MTMs, we wanted to correlate the
237 macrophage status with their localization and performed *in situ* stainings to identify
238 whether intra-epithelial macrophages in early lesions might be CD206^{hi} MTMs as well.
239 To this end we co-stained wild type glands, early lesions and overt tumors tissues
240 against F4/80 and CD206 (**Fig.5K-M**). We found that stromal and intra-epithelial
241 macrophages in both wild type glands and early lesions were CD206^{hi} whereas tumor

242 associated macrophages in overt tumors were CD206^{lo} (**Fig.5N**). While tracing the
243 exact origin and lineage of macrophage subtypes will require further scrutiny, our data
244 suggest that intra-epithelial macrophages might be derived from resident mammary
245 tissue macrophages and that expansion of monocyte derived tumor associated
246 macrophages is a hallmark of overt tumor stages.

247

248 **HER2+ EARLY CANCER CELLS PRODUCE CCL2 AND RECRUIT MACROPHAGES INTO MAMMARY**
249 **DUCTS.**

250 We next explored what signals might HER2 upregulation induce that might attract
251 resident mammary tissue macrophages from the stroma into the ductal epithelium of
252 HER2+ early lesions. In invasive breast cancer models, HER2 signaling activates NFκB,
253 which transcriptionally induces CCL2, a potent macrophage chemotactic factor ³².
254 Accordingly, the p65 subunit of NFκB subunit was phosphorylated in mammospheres
255 derived from HER2+ early cancer cells, and Lapatinib, a HER2 and EGFR inhibitor,
256 inhibited its phosphorylation (**Fig.6A**). We then isolated RNA from mammospheres
257 derived from either FVB wild type or MMTV-HER2 early MIN lesions as described ³³ and
258 performed quantitative real-time PCR analysis for cytokine mRNAs. We found that
259 already at these early stages of progression, when enhanced proliferation is not yet
260 detectable ²⁴, HER2+ cancer cells upregulated expression of CCL2 but not CSF2,
261 CSF1, IL1β, and IL6 (**Fig. 6B, Supplementary Fig.4A,B**). Upregulation of CCL2 around
262 HER2+ early cancer cells was also observed at the protein levels as revealed by
263 immunofluorescence (**Fig.6C,D, Supplementary Fig.4C-E**). CCR2+ cells could be
264 found close to CCL2+ early cancer cells (**Fig.6C insert**). Additionally, acinar-like

265 structures produced by early MMTV-HER2 cancer cells displayed a reduction in
266 secreted and peri-organoid CCL2 production upon inhibition of HER2 or NFkB signaling
267 with specific inhibitors³⁴ (**Fig.6E-G**). To confirm that CCL2 signaling was necessary and
268 sufficient for HER2-dependent macrophage recruitment, HER2+ early cancer cells were
269 grown as 3D acinar structures *in vitro* for 5 days. Cultures were then treated with
270 Lapatinib, an IKK β inhibitor³⁴ or an inhibitor of the CCL2 receptor CCR2 (RS504393)
271 and macrophages isolated from mammary glands of MMTV-HER2 mice were added to
272 the cultures. After 24 hours of co-culture, macrophages were associated with ~50% of
273 all organoid structures in control samples (**Fig.6H**). In contrast, co-cultures treated with
274 the inhibitors all showed significant reduction in macrophage association (**Fig.6I,J**). We
275 next treated 20 week old MMTV-HER2 mice carrying only early lesions (no palpable or
276 overt tumors) for 2 weeks with a CCR2 inhibitor (**Fig.6K,L**). We found that the number
277 of intra-epithelial macrophages was significantly reduced when mice were treated
278 systemically (**Fig.6M**). When the CCR2 inhibitor was administered locally into the fat
279 pad to avoid systemic effects (**Fig.6N**), intra-epithelial macrophage content was reduced
280 compared to contra-lateral control treated glands (**Fig.6O**), supporting that intra-
281 epithelial macrophages are indeed derived from resident mammary gland macrophages
282 instead of circulating monocyte derived macrophages. Additionally, mammary tissue
283 macrophages can also be depleted by genetic ablation of CCR2³¹ arguing that we may
284 be eliminating the same population during early mammary cancer stages. We conclude
285 that HER2 signaling in cancer cells from early lesions activates NFkB to induce CCL2,
286 which in turn mobilizes CCR2+ resident mammary macrophages from the stroma into
287 these early lesions.

288 **HIGH INTRA-EPITHELIAL MACROPHAGE NUMBERS IN PATIENT DCIS LESIONS CORRELATE WITH**
289 **LOW E-CADHERIN LEVELS.**

290 Published data showed that more than 10% of patients with DCIS had detectable
291 DCCs in their bone marrow (BM), but no histologic markers, which include invasive
292 fronts and receptor status were indicative of the presence of DCCs ³. To test whether
293 macrophages could also infiltrate early lesions in humans, we compared macrophages
294 in healthy human breast tissue vs. tissue from DCIS lesions as a model of early stage
295 breast cancer lesions. Macrophages were identified as CD68+/CD45+ and
296 cytokeratin8/18 negative cells (**Supplementary Fig.5A,B**). In breast tissue from healthy
297 donors, macrophages were localized in the stroma in the vicinity of mammary ducts but
298 remained outside of the ducts, which were delimited by an intact myoepithelial layer of
299 cells (**Fig.7A**). In contrast, even in DCIS lesions that displayed an apparently intact
300 myoepithelial layer, there was a statistically significant increase in the frequency of
301 macrophages found inside the aberrant ductal epithelial structure in between cancer
302 cells (**Fig.7B,C**). The association of intra-epithelial macrophages with reduced E-
303 Cadherin levels was confirmed in human DCIS samples (N=12). This was independent
304 of HER2 status and appeared in different patterns. Patients with high macrophage
305 numbers within lesions showed overall lower E-Cadherin levels as measured by
306 quantitative image analysis (**Fig.7D-F**). Additionally, within the same patient, individual
307 lesions with high macrophage numbers had lower E-Cadherin levels (**Supplementary**
308 **Fig.5C-E**). This reveals an inter- and intra-tumor heterogeneity and suggests that some
309 regions of DCIS lesions might be more prone to contain cancer cells able to undergo
310 early dissemination.

311 **Discussion**

312 Following the assumption that dissemination occurs only during late invasive cancer
313 stages, many studies have focused on investigating dissemination from invasive
314 lesions. However, micro-invasion events were detected in patients' "pre-invasive" DCIS
315 lesions using electron microscopy, but these events might go unnoticed by light
316 microscopy ⁶. Additionally, DCIS lesions were found to be vascularized ³⁵, indicating
317 that there might be a possibility for early cancer cell dissemination within the DCIS
318 lesions. Our data reveal that macrophages enter the epithelium of early lesions in mice
319 and human DCIS where they create early dissemination microenvironments. In mice
320 this process can be initiated by the HER2 oncogene before growth stimulation is
321 evident, revealing a novel function for the HER2 oncogene that could be targeted. The
322 HER2 orchestrated early dissemination microenvironments contain early cancer cells
323 that attract CCR2+ macrophages *via* CCL2 secretion that in turn secrete Wnt-1 to
324 dismantle epithelial E-Cadherin junctions. The dissemination-promoting function of
325 macrophages was proven when we found that depletion of macrophages in early
326 HER2+ lesions using anti-CSF1R antibodies reversed the loss of E-cadherin in HER2+
327 lesions as well as intravasation and dissemination to lungs. Interestingly, Wnt signaling
328 is linked to branching morphogenesis ^{36,37} and a subset of tumor-associated
329 macrophages that drive invasive cancer dissemination also secrete Wnt ligands ²⁷.

330 We found that the myelo-monocytic landscape of HER2+ early lesions at the time
331 of early dissemination resembled that of healthy mammary glands and largely consisted
332 of M2 polarized F4/80+/CD11b+/CD206+/Tie2+ macrophages. In contrast, overt tumors
333 predominantly contained CD11b^{int}/CD206^{lo}/Tie2^{lo}/VCAM+ macrophages as described ³¹

334 but these were the minority of macrophages in wild type and early lesion ducts. We
335 corroborated these findings *in situ* by immunofluorescence staining, confirming that
336 intra-epithelial macrophages and wild type resident macrophages are CD206+ whereas
337 tumor associated macrophages are CD206^{lo}. Interestingly, the profile of resident and
338 early lesion macrophages is characteristic for a subset of macrophages in invasive
339 breast cancer lesions that are gatekeepers of intravasation doorways ¹⁹.

340 This raises the possibility that when HER2 is overexpressed in mammary
341 epithelial cells, resident macrophages have the inherent potential to aberrantly fuel
342 epithelial cell motility as is the case during physiologic mammary gland development
343 ^{17,18,29}. While the barrier between stroma and epithelium prevents resident macrophages
344 from disrupting the steady state epithelial architecture, oncogene-activated attraction of
345 resident macrophages into the epithelium might result in disruption of normal tissue
346 boundaries and early dissemination. However, further scrutiny and lineage tracing
347 experiments are required to fully understand the origin of macrophages driving early
348 and late dissemination.

349 We further found that when macrophages were depleted during early stages but
350 allowed to rebound during invasive stages, lung metastatic burden was still reduced.
351 This indicates that early DCCs contribute to lung metastasis formation, either directly or
352 indirectly and surprisingly large tumors that persisted in mice for ~1.5 months were not
353 able to compensate for the reduced dissemination during early stages. While the exact
354 clinical implications of our findings need further analysis, a few scenarios of clinical
355 relevance can be discussed. It is argued that because 13% of DCIS patients show
356 disseminated disease and only 3% develop metastatic disease ⁸⁻¹², early dissemination

357 is not a contributor to lethal metastatic cancer. However, approximately 50% of breast
358 cancer deaths after DCIS occurred in the absence of a detectable local invasive disease
359 and were not influenced by current treatments ¹⁰. Further, cancer can manifest with
360 metastasis without a detectable primary even after careful inspection of the patients ³⁸.
361 These clinical findings indicate that at least in a subgroup of patients, early DCCs may
362 develop lethal metastases ¹⁰ (**Fig.7G** scenario 1). Additionally, early DCCs may
363 cooperate with later arriving DCCs to form metastasis in patients that after DCIS
364 treatment go on to develop invasive lesions or in patients that had DCIS but only were
365 diagnosed later for invasive cancer (**Fig.7G** scenario 2). This resembles the concept of
366 the “pre-metastatic” niche described previously ^{39,40} where the pre-metastatic niche
367 could also be orchestrated by early DCCs. Next phase studies will address the genetic
368 identity of metastasis affected by macrophage depletion and determine the contribution
369 of early DCCs to the metastatic burden late in cancer progression.

370 Overall, our studies suggest that before propelling rapid growth, oncogenes such
371 as HER2 might turn on developmental programs of anoikis resistance ²⁴, macrophage
372 recruitment and invasion that initiate dissemination much earlier than anticipated. We
373 provide critical new insight into the understanding of the natural history of metastatic
374 disease and we demonstrate that macrophages and early DCCs appear to play a
375 seminal role in metastatic breast cancer.

376

377 **Methods.**

378 **Cells and cell culture.** Raw264.7 cells expressing mCherry were generated using
379 mCherry lentiviral vectors and maintained in DMEM (Lonza) with 10% FBS and 1%

380 Pen/Strep. Comma-1D cells were maintained in DMEM-F12 medium containing
381 2%FBS, 1% Pen/Strep. For DKK1 stimulation, conditioned media was prepared from
382 DKK1 expressing 293T cells and protein concentration was determined using a
383 Bradford assay cells cultured with serum free medium (DMEM + 1%P/S) for 24 hours
384 and then concentrated using Vivaspin 20 Centrifugal Concentrating tubes (Sartorius,
385 VS2021) at 3000g up to 3 hours until desired concentration (10x) was reached.
386 0.5ug/ml DKK1 protein was used for stimulation. For co-culture experiments, Comma-
387 1D cells were seeded on coverslips and after 12h, Raw-264.7-mCherry cells were
388 added. Co-cultures were fixed in 2% formalin after 12h and then stained. All cell lines
389 were routinely tested for mycoplasma.

390

391 **Mouse experiments.** All animal procedures were approved by the Institutional Animal
392 Care and Use Committee (IACUC) of Icahn School of Medicine at Mount Sinai,
393 protocols 08-0366 and 2014-0190. FVB/N-Tg(MMTVneu)202Mul/J or FVB wild
394 type mice were purchased from Jackson laboratory and bred in-house.
395 Animals were sacrificed using CO₂ at age 14, 20-22wk or when invasive tumors had
396 reached a diameter of 1cm. For macrophage depletion, we administered 3mg of the
397 CSF1R antibody clone ASF98 on day 1 and 1mg on day 7 and weekly thereafter by
398 injection into the tail vein of 18wk old pre-malignant MMTV-Her2 mice. PBS was used
399 as vehicle control. Treatment lasted 14 days or until tumors were first palpable (3mm
400 diameter). ASF98 antibody was a generous gift of Dr. Miriam Merad. For CCR2
401 blockade, mice were either treated with 2mg/kg of RS504393 (Tocris Bioscience) or

402 vehicle control (DMSO) daily by i.p. injections for 14 days or by injection of 1mg/kg
403 RS504393 into the fat pad for 5d.

404 **Mammary Gland Whole Mounts.** Mammary glands were excised, fixed in Carnoy's
405 fixative and stained in carmine alum solution as described
406 in <http://mammary.nih.gov/tools/histological/Histology/index.html>.

407 **Microscopy.** Formalin fixed and paraffin embedded samples were prepared and
408 stained as described ⁴¹. For immunohistochemistry, VectaStain Elite ABC Rabbit IgG
409 and Mouse IgG (PK-6102) kits from Vector Laboratories were used for secondary
410 antibodies. Secondary antibodies were left for one hour at room temperature. DAB and
411 Vector Blue substrate kit (Vector Laboratories) were used for enzymatic substrate.
412 Mounting was done using VECTASHIELD mounting media (Vector Laboratories). For
413 CD206 stainings, cryosections were used. Tissue was fixed in 4% formalin over night,
414 incubated in 30% sucrose/PBS over night and sectioned into 6mm sections. Staining of
415 cryosection was done as described ⁴². Antibodies used were: CD68 (Sigma, polyclonal),
416 F4/80 (abcam CIA:3-1), Iba-1 (Wako polyclonal), Cytokeratin 8/18 (Progen, polyclonal),
417 smooth muscle actin (Sigma IA4), CD206 (Biolegend C068C2), CCL2 (Novus 2D8), E-
418 Cadherin (Becton Dickinson, polyclonal), beta catenin (cell signaling, polyclonal), Her2
419 (abcam, polyclonal), Endomucin (Santa Cruz 7C7). For costaining of F4/80 and CD206
420 (both raised in rat) a FITC-conjugated F4/80 antibody (Biolegend BM8) was used in
421 combination with CD206 (Biolegend C068C2) in a sequential stain. Microscopic
422 analysis was carried out with a Leica widefield microscope or with a Leica confocal
423 microscope for 3D cultures. For quantification of immunofluorescence signal intensity
424 with the Metamorph software, regions of interest were defined in original tiff files that

425 had been taken under the same exposure time and settings and the mean signal
426 intensity was measured. Because the use of a directly conjugated F4/80 antibody
427 resulted in lower signal intensity, we used Iba1 as a macrophage marker ¹⁹ to identify
428 macrophages for CD206 signal intensity measurement instead.

429

430 **Flow Cytometry.** MMTV-HER2 mice were sacrificed using CO₂ at age 18-22wk (early
431 pre-malignant cancer lesions) or when overt tumors had formed. Whole mammary
432 glands or tumors were digested in Collagenase/BSA at 37°C for 30-45min. Red blood
433 cell lysis buffer (Sigma) was used to remove blood cells. Cell suspensions were blocked
434 with Fc-blocking reagent (eBioscience) and samples were surface stained in FACS
435 buffer (PBS supplemented with 1% BSA and 2mM EDTA) for 20-30 min on ice using the
436 following antibodies: CD45-PerCPy5.5 (Biolegend 30-F11), CD11b-PeCy7
437 (eBioscience M1/70), CD11c-PE (eBioscience N418), Gr1-AF700 (eBioscience
438 RB68C5), Tie2-biotin (eBioscience TEK4), F4/80-biotin (Biolegend BM8), CD206-APC
439 (Biolegend C068C2), VCAM-FITC (eBioscience 429). DAPI was used to label dead
440 cells. Multiparameter analysis was performed on a Fortessa (BD) and analyzed with
441 FlowJo software (Tree Star). DAPI+ cells and doublets were excluded from all analysis.
442 To sort mammary tissue macrophages, whole mammary glands from 14wk, 18-22wk
443 (early pre-malignant cancer lesions) mammary glands or from invasive tumors were
444 digested in Collagenase/BSA at 37°C for 30-45min. Mononuclear cells were enriched in
445 a Percoll gradient and then macrophages were sorted as viable CD45+/Gr1-
446 /CD11b+/F4/80+ cells.

447

448 **CyTOF analysis.** All mass cytometry reagents were purchased from Fluidigm Inc.
449 (former DVS) unless otherwise noted. Mice were injected i.p. with 1mg IdU per mouse
450 16h prior to the experiment. Lymph nodes were removed and mammary glands were
451 digested using the Miltenyi fatty tissue digestion kit. Cells were then washed with PBS
452 containing 1% BSA and blocked with Fc-blocking reagent (eBioscience) to minimize
453 non-specific antibody binding. Cells were stained with a panel of metal-labeled
454 antibodies against 20 cell surface markers (Fig.5 supplement 1A) for 30 minutes on ice,
455 and then washed. All antibodies were either purchased pre-conjugated to metal tags, or
456 conjugated in-house using MaxPar X8 conjugation kits according to the manufacturer's
457 instructions. After antibody staining, cells were incubated with cisplatin for 5 minutes at
458 RT as a viability dye for dead cell exclusion. Cells were then fixed and permeabilized
459 with a commercial fix/perm buffer (BD Biosciences) and stored in PBS containing 1.6%
460 formaldehyde and a 1:4000 dilution of Ir nucleic acid intercalator to label all nucleated
461 cells. Immediately prior to acquisition, cells were washed in PBS, and diH₂O and
462 resuspended in diH₂O containing a 1/10 dilution of EQ 4 Element Calibration beads.
463 After routine instrument tuning and optimization, the samples were acquired on a
464 CyTOF2 Mass Cytometer in sequential 10min acquisitions at an acquisition rate of <500
465 events/s. The resulting FCS files were concatenated and normalized using a bead-
466 based normalization algorithm in the CyTOF acquisition software and analyzed with
467 Cytobank. FCS files were manually pre-gated on Ir193 DNA⁺ CD45⁺ events, excluding
468 dead cells, doublets and DNA-negative debris. Myeloid derived cells were manually
469 gated based on CD11c and CD11b expression and the gated myeloid populations were
470 then analyzed using viSNE³⁰ based on all myeloid phenotypic markers. Putative cell

471 populations on the resulting viSNE map were manually gated based on the expression
472 of canonical markers, while allowing for visualization of additional heterogeneity within
473 and outside of the labeled population bubbles.

474

475 **Mammospheres and 3D mammary primary epithelial cell cultures.** Acini cultures
476 were performed as described ^{33,43}. 5×10^4 eCCs were seeded in in 400ul Assay
477 Medium in 8-well chamber slides coated with 40ul of Matrigel (Corning). Acini formed at
478 an efficiency of around 30 acini/ 1×10^4 MECs plated. For macrophage co-cultures,
479 primary tissue macrophages were added at a ratio of 500 per 1×10^4 eCCs seeded to 5d
480 old acini cultures. For inhibitory treatments, 5d old acini cultures were treated for 24h
481 with $1 \mu\text{M}$ Lapatinib (LC Laboratories), $2 \mu\text{M}$ IKK Inhibitor ³⁴ (generous gift from Dr. Albert
482 Baldwin), $1 \mu\text{M}$ CCR2 inhibitor RS504393 (Tocris Bioscience) or DMSO as vehicle
483 control. Cultures were then fixed for immunofluorescence (IF) with 4% PFA.
484 Mammosphere cultures were prepared as described ³³. To prepare conditioned
485 medium, 5d old mammosphere culture were plated in serum free DMEM medium and
486 conditioned medium was harvested after 24h.

487

488 **Immunoblotting, RT-PCR, and quantitative PCR (qPCR).** Immunoblotting was
489 performed as described previously ^{44,45}. Antibodies used were P-NF-kappa-B p65 (Cell
490 Signaling polyclonal) and beta-tubulin (abcam, polyclonal). For expression analysis of
491 FVB wild type mammary epithelial cells or MMTV-Her2 eCCs, epithelial cells were
492 isolated and grown as mammospheres for 5d as described ³³. For expression analysis
493 of Raw264.7 macrophages, cells were grown as monolayers in 6-well culture dishes

494 and treated with conditioned medium for 24h. RNA isolation was performed using Trizol
495 (Life Technologies) or the RNeasy Kit (Qiagen) for MTMs. RT- and qPCR were
496 performed as described ⁴¹. All samples were normalized to GAPDH expression and 2⁻
497 $\Delta\Delta C_t$ values were calculated as described ⁴⁶. Primers were purchased from IDT.
498 Primer sequences were: Mouse- GAPDH forward primer 5'-
499 AACTTTGGCATTGTGGAAGGGCTC-3'; GAPDH reverse primer 5'-
500 TGGAAGAGTGGGAGTTGCTGTTGA-3. E-Cadherin forward primer 5'-
501 CAAGGACAGCCTTCTTTTCG-3'; E-Cadherin reverse primer 5'-
502 TGGACTTCAGCGTCACTTTG-3'. Wnt-1 forward primer 5'-
503 CAGTGAAGGTGCAGTTGCAG-3'; Wnt-1 reverse primer 5'-
504 CAGTGAAGGTGCAGTTGCAGC-3'. CSF1 forward primer 5'-
505 CAACAGCTTTGCTAAGTGCTCTA-3'; CSF1 reverse primer 5'-
506 CACTGCTAGGGGTGGCTTTA-3'. CCL2 forward primer 5'-
507 GGCTGGAGAGCTACAAGAGG-3'; CCL2 reverse primer 5'-
508 GGTCAGCACAGACCTCTCTC-3'.

509 **Patient samples.** Paraffin embedded sections from patients with DCIS were obtained
510 from the Cancer Biorepository at Icahn School of Medicine at Mount Sinai, New York,
511 NY and from Thomas Karn, University of Frankfurt, Germany. Samples were fully de-
512 identified and obtained with Institutional Review Board approval, which indicated that
513 this work does not meet the definition of human subject research according to the 45
514 CFR 46 and the Office of Human Subject Research.

515 **Circulating Cancer Cells (CCCs) and Disseminated Cancer Cells (DCCs)**
516 **detection.** For CCC analysis, blood was drawn by cardiac puncture following IACUC
517 protocols. CCCs were purified using negative lineage cell-depletion kit (Miltenyi), fixed
518 with 3% PFA for 20 min on ice and cytopsin preparations were carried out by
519 centrifugation of blood cells at 500 rpm for 3 min using poly-L-lysine-coated slides
520 (Sigma).

521 **Statistical Analysis.** Unless noted otherwise, all of the experiments presented in the
522 manuscript were repeated at least 3 times with replicates of at least 3. Statistical
523 Analysis was done using Graph Pad Prism Software. For all cell culture experiments
524 (experiments with technical replicates), one-tailed *student t-tests* were performed. For
525 mouse experiments, *Mann-Whitney* tests were used. Differences were considered
526 significant if *P* values were ≤ 0.05 .

527

528 **References.**

- 529 1 Turajlic, S. & Swanton, C. Metastasis as an evolutionary process. *Science* **352**,
530 169-175, doi:10.1126/science.aaf2784 (2016).
- 531 2 Braun, S. *et al.* A pooled analysis of bone marrow micrometastasis in breast
532 cancer. *The New England journal of medicine* **353**, 793-802,
533 doi:10.1056/NEJMoa050434 (2005).
- 534 3 Banys, M. *et al.* Hematogenous and lymphatic tumor cell dissemination may be
535 detected in patients diagnosed with ductal carcinoma in situ of the breast. *Breast*
536 *cancer research and treatment* **131**, 801-808, doi:10.1007/s10549-011-1478-2
537 (2012).
- 538 4 Schardt, J. A. *et al.* Genomic analysis of single cytokeratin-positive cells from
539 bone marrow reveals early mutational events in breast cancer. *Cancer cell* **8**,
540 227-239, doi:10.1016/j.ccr.2005.08.003 (2005).
- 541 5 Sanger, N. *et al.* Disseminated tumor cells in the bone marrow of patients with
542 ductal carcinoma in situ. *Int J Cancer* **129**, 2522-2526, doi:10.1002/ijc.25895
543 (2011).
- 544 6 Husemann, Y. *et al.* Systemic spread is an early step in breast cancer. *Cancer*
545 *cell* **13**, 58-68, doi:10.1016/j.ccr.2007.12.003 (2008).

546 7 Pavlidis, N., Khaled, H. & Gaafar, R. A mini review on cancer of unknown primary
547 site: A clinical puzzle for the oncologists. *Journal of advanced research* **6**, 375-
548 382, doi:10.1016/j.jare.2014.11.007 (2015).

549 8 Cutuli, B. *et al.* Ductal carcinoma in situ of the breast results of conservative and
550 radical treatments in 716 patients. *Eur J Cancer* **37**, 2365-2372 (2001).

551 9 Donker, M. *et al.* Breast-conserving treatment with or without radiotherapy in
552 ductal carcinoma In Situ: 15-year recurrence rates and outcome after a
553 recurrence, from the EORTC 10853 randomized phase III trial. *Journal of clinical
554 oncology : official journal of the American Society of Clinical Oncology* **31**, 4054-
555 4059, doi:10.1200/JCO.2013.49.5077 (2013).

556 10 Narod, S. A., Iqbal, J., Giannakeas, V., Sopik, V. & Sun, P. Breast Cancer
557 Mortality After a Diagnosis of Ductal Carcinoma In Situ. *JAMA oncology*,
558 doi:10.1001/jamaoncol.2015.2510 (2015).

559 11 Warnberg, F., Bergh, J., Zack, M. & Holmberg, L. Risk factors for subsequent
560 invasive breast cancer and breast cancer death after ductal carcinoma in situ: a
561 population-based case-control study in Sweden. *Cancer epidemiology,
562 biomarkers & prevention : a publication of the American Association for Cancer
563 Research, cosponsored by the American Society of Preventive Oncology* **10**,
564 495-499 (2001).

565 12 Warnberg, F. *et al.* Effect of radiotherapy after breast-conserving surgery for
566 ductal carcinoma in situ: 20 years follow-up in the randomized SweDCIS Trial.
567 *Journal of clinical oncology : official journal of the American Society of Clinical
568 Oncology* **32**, 3613-3618, doi:10.1200/JCO.2014.56.2595 (2014).

569 13 Eyles, J. *et al.* Tumor cells disseminate early, but immunosurveillance limits
570 metastatic outgrowth, in a mouse model of melanoma. *The Journal of clinical
571 investigation* **120**, 2030-2039, doi:10.1172/JCI42002 (2010).

572 14 Rhim, A. D. *et al.* EMT and dissemination precede pancreatic tumor formation.
573 *Cell* **148**, 349-361, doi:10.1016/j.cell.2011.11.025 (2012).

574 15 Liu, Y. J. *et al.* Confinement and low adhesion induce fast amoeboid migration of
575 slow mesenchymal cells. *Cell* **160**, 659-672, doi:10.1016/j.cell.2015.01.007
576 (2015).

577 16 Nguyen-Ngoc, K. V. *et al.* ECM microenvironment regulates collective migration
578 and local dissemination in normal and malignant mammary epithelium. *Proc Natl
579 Acad Sci U S A* **109**, E2595-2604, doi:10.1073/pnas.1212834109 (2012).

580 17 Van Nguyen, A. & Pollard, J. W. Colony stimulating factor-1 is required to recruit
581 macrophages into the mammary gland to facilitate mammary ductal outgrowth.
582 *Developmental biology* **247**, 11-25, doi:10.1006/dbio.2002.0669 (2002).

583 18 Gouon-Evans, V., Rothenberg, M. E. & Pollard, J. W. Postnatal mammary gland
584 development requires macrophages and eosinophils. *Development* **127**, 2269-
585 2282 (2000).

586 19 Harney, A. S. *et al.* Real-Time Imaging Reveals Local, Transient Vascular
587 Permeability, and Tumor Cell Intravasation Stimulated by TIE2hi Macrophage-
588 Derived VEGFA. *Cancer discovery*, doi:10.1158/2159-8290.CD-15-0012 (2015).

589 20 Wyckoff, J. *et al.* A paracrine loop between tumor cells and macrophages is
590 required for tumor cell migration in mammary tumors. *Cancer research* **64**, 7022-
591 7029, doi:10.1158/0008-5472.CAN-04-1449 (2004).

- 592 21 Liu, C. Y. *et al.* M2-polarized tumor-associated macrophages promoted epithelial-
593 mesenchymal transition in pancreatic cancer cells, partially through TLR4/IL-10
594 signaling pathway. *Laboratory investigation; a journal of technical methods and*
595 *pathology* **93**, 844-854, doi:10.1038/labinvest.2013.69 (2013).
- 596 22 Bonde, A. K., Tischler, V., Kumar, S., Soltermann, A. & Schwendener, R. A.
597 Intratumoral macrophages contribute to epithelial-mesenchymal transition in solid
598 tumors. *BMC cancer* **12**, 35, doi:10.1186/1471-2407-12-35 (2012).
- 599 23 Cardiff, R. D. Validity of mouse mammary tumour models for human breast
600 cancer: comparative pathology. *Microscopy research and technique* **52**, 224-230,
601 doi:10.1002/1097-0029(20010115)52:2<224::AID-JEMT1007>3.0.CO;2-A
602 (2001).
- 603 24 Wen, H. C. *et al.* p38alpha Signaling Induces Anoikis and Lumen Formation
604 During Mammary Morphogenesis. *Science signaling* **4**, ra34,
605 doi:10.1126/scisignal.2001684 (2011).
- 606 25 Wang, S. *et al.* Wnt1 positively regulates CD36 expression via TCF4 and PPAR-
607 gamma in macrophages. *Cellular physiology and biochemistry : international*
608 *journal of experimental cellular physiology, biochemistry, and pharmacology* **35**,
609 1289-1302, doi:10.1159/000373951 (2015).
- 610 26 Cosin-Roger, J. *et al.* M2 macrophages activate WNT signaling pathway in
611 epithelial cells: relevance in ulcerative colitis. *PloS one* **8**, e78128,
612 doi:10.1371/journal.pone.0078128 (2013).
- 613 27 Ojalvo, L. S., Whittaker, C. A., Condeelis, J. S. & Pollard, J. W. Gene expression
614 analysis of macrophages that facilitate tumor invasion supports a role for Wnt-
615 signaling in mediating their activity in primary mammary tumors. *J Immunol* **184**,
616 702-712, doi:10.4049/jimmunol.0902360 (2010).
- 617 28 Stanley, E. R., Cifone, M., Heard, P. M. & Defendi, V. Factors regulating
618 macrophage production and growth: identity of colony-stimulating factor and
619 macrophage growth factor. *The Journal of experimental medicine* **143**, 631-647
620 (1976).
- 621 29 Gouon-Evans, V., Lin, E. Y. & Pollard, J. W. Requirement of macrophages and
622 eosinophils and their cytokines/chemokines for mammary gland development.
623 *Breast cancer research : BCR* **4**, 155-164 (2002).
- 624 30 Amir el, A. D. *et al.* viSNE enables visualization of high dimensional single-cell
625 data and reveals phenotypic heterogeneity of leukemia. *Nature biotechnology* **31**,
626 545-552, doi:10.1038/nbt.2594 (2013).
- 627 31 Franklin, R. A. *et al.* The cellular and molecular origin of tumor-associated
628 macrophages. *Science* **344**, 921-925, doi:10.1126/science.1252510 (2014).
- 629 32 Cogswell, P. C., Guttridge, D. C., Funkhouser, W. K. & Baldwin, A. S., Jr.
630 Selective activation of NF-kappa B subunits in human breast cancer: potential
631 roles for NF-kappa B2/p52 and for Bcl-3. *Oncogene* **19**, 1123-1131,
632 doi:10.1038/sj.onc.1203412 (2000).
- 633 33 Cohn, E., Ossowski, L., Bertran, S., Marzan, C. & Farias, E. F. RARalpha1
634 control of mammary gland ductal morphogenesis and wnt1-tumorigenesis. *Breast*
635 *cancer research : BCR* **12**, R79, doi:10.1186/bcr2724 (2010).

636 34 Basseres, D. S., Ebbs, A., Cogswell, P. C. & Baldwin, A. S. IKK is a therapeutic
637 target in KRAS-Induced lung cancer with disrupted p53 activity. *Genes & cancer*
638 **5**, 41-55 (2014).

639 35 Cocker, R., Oktay, M. H., Sunkara, J. L. & Koss, L. G. Mechanisms of
640 progression of ductal carcinoma in situ of the breast to invasive cancer. A
641 hypothesis. *Medical hypotheses* **69**, 57-63, doi:10.1016/j.mehy.2006.11.042
642 (2007).

643 36 Brisken, C. *et al.* Essential function of Wnt-4 in mammary gland development
644 downstream of progesterone signaling. *Genes & development* **14**, 650-654
645 (2000).

646 37 Robinson, G. W., Hennighausen, L. & Johnson, P. F. Side-branching in the
647 mammary gland: the progesterone-Wnt connection. *Genes & development* **14**,
648 889-894 (2000).

649 38 Pavlidis, N. & Fizazi, K. Cancer of unknown primary (CUP). *Critical reviews in*
650 *oncology/hematology* **54**, 243-250, doi:10.1016/j.critrevonc.2004.10.002 (2005).

651 39 Kaplan, R. N. *et al.* VEGFR1-positive haematopoietic bone marrow progenitors
652 initiate the pre-metastatic niche. *Nature* **438**, 820-827, doi:10.1038/nature04186
653 (2005).

654 40 Peinado, H. *et al.* Melanoma exosomes educate bone marrow progenitor cells
655 toward a pro-metastatic phenotype through MET. *Nature medicine* **18**, 883-891,
656 doi:10.1038/nm.2753 (2012).

657 41 Bragado, P. *et al.* TGF-beta2 dictates disseminated tumour cell fate in target
658 organs through TGF-beta-RIII and p38alpha/beta signalling. *Nature cell biology*
659 **15**, 1351-1361, doi:10.1038/ncb2861 (2013).

660 42 Lederle, W. *et al.* Platelet-derived growth factor-B normalizes micromorphology
661 and vessel function in vascular endothelial growth factor-A-induced squamous
662 cell carcinomas. *The American journal of pathology* **176**, 981-994,
663 doi:10.2353/ajpath.2010.080998 (2010).

664 43 Debnath, J., Muthuswamy, S. K. & Brugge, J. S. Morphogenesis and
665 oncogenesis of MCF-10A mammary epithelial acini grown in three-dimensional
666 basement membrane cultures. *Methods* **30**, 256-268 (2003).

667 44 Adam, A. P. *et al.* Computational identification of a p38SAPK-regulated
668 transcription factor network required for tumor cell quiescence. *Cancer research*
669 **69**, 5664-5672, doi:10.1158/0008-5472.CAN-08-3820 (2009).

670 45 Ranganathan, A. C., Zhang, L., Adam, A. P. & Aguirre-Ghiso, J. A. Functional
671 coupling of p38-induced up-regulation of BiP and activation of RNA-dependent
672 protein kinase-like endoplasmic reticulum kinase to drug resistance of dormant
673 carcinoma cells. *Cancer research* **66**, 1702-1711, doi:10.1158/0008-5472.CAN-
674 05-3092 (2006).

675 46 Livak, K. J. & Schmittgen, T. D. Analysis of relative gene expression data using
676 real-time quantitative PCR and the 2(-Delta Delta C(T)) Method. *Methods* **25**,
677 402-408, doi:10.1006/meth.2001.1262 (2001).

678

679

680 **Author Contributions.**

681 N.L. designed and optimized experimental approach, performed *in vitro* and *in vivo*
682 experiments, analyzed data and co-wrote the manuscript, A.M. and A.R. and the
683 Human Immune Monitoring Core performed CyTOF experiments, E.F., M.S.S., E.T.,
684 and K.H. performed experiments, M.M. provided general guidance and oversight and
685 co-wrote the manuscript, J.A.A.-G. designed and optimized experimental approach,
686 provided general guidance and oversight, analyzed data and co-wrote the manuscript.

687

688 **Acknowledgments.**

689 We thank the Aguirre-Ghiso and the Merad labs for helpful discussion. We are grateful
690 to A. Baldwin for providing the IKK inhibitor. We thank J. Ochando and the Flow
691 Cytometry Core for technical support and assistance with cell sorting. N.L. was funded
692 by DFG fellowship Li23561-1 and DoD-BrCRP BC133807 and J.A.A.-G. was funded by
693 NIH/National Cancer Institute (CA109182, CA163131).

694

695 **Author information.**

696 The authors declare no competing financial interests.

697

698

699 **Figure Legends.**

700

701 **Figure 1: Macrophages enter the ductal epithelial layer in early breast cancer**
702 **lesions.** HE stainings of mammary gland sections show progression from healthy
703 mammary ducts in FVB wild type glands (**A**) to early lesions classified as hyperplasia
704 and mammary intra-epithelial neoplasia (**B**) to invasive tumors (**C**) in the MMTV-HER2
705 mouse model. Mammary glands from FVB wild type (**D**) of pre-malignant MMTV-HER2
706 mice at age 14 (**E**) and 22 (**F**) weeks were stained against F4/80 (macrophages) and
707 CK8/18 (epithelial cells) and against F4/80 and SMA (**E-G**). Bars 10 μ m. The mean plus
708 SEM of the percentage of ducts containing IEM is shown; each dot represents one
709 animals (**H**).

710

711 **Figure 2: Intra-epithelial macrophages induce an EMT-like response in early**
712 **cancer cells.** 20wk old MMTV-HER2 mouse mammary glands were stained against E-
713 Cadherin and F4/80. E-Cadherin localization was analyzed dependent on whether
714 macrophages did not make direct contact to the duct (no M. or distant M.; **A**) or whether
715 ducts contain intra-epithelial macrophages (IEM; **B**). The percentage of individual
716 epithelial cells that showed disrupted E-Cadherin (arrow in B) was quantified (**C**). Plot
717 shows means plus SEM; each dot represents one animal. E-Cadherin mRNA
718 expression in whole mammary glands of FVB wild type (WT) or 20wk old MMTV-HER2
719 mice was determined by qPCR. Plot (**D**) shows means plus SEM; each dot represents
720 one animal. 24wk old MMTV-HER2 mammary glands were stained against β -Catenin
721 and Iba1, a macrophage marker (**E,F**). β -Catenin+ early cancer cells (blue arrows in F)

722 were more frequent in ducts containing intra-epithelial macrophages (black arrows in F)
723 (G). Each dot represents one animal, plots show mean plus SEM. The mammary
724 epithelial cell line Comma-1D was grown as a monolayer and Raw264.7 macrophages
725 stably transfected with mCherry were added. After 12h, co-cultures were stained
726 against E-Cadherin (H) or β -Catenin (I) and the signal intensity of β -Catenin signals
727 inside individual nuclei was quantified (J). Boxplot shows range of nuclear β -catenin
728 signal intensity in individual cells; independent experiments N=3. (K,L) Conditioned
729 medium was harvested from primary cultures of wild type (WT) or pre-malignant MMTV-
730 HER2 mammospheres and added to Raw264.7 macrophages or mammary tissue
731 macrophages (MTMs) isolated from pre-malignant MMTV-HER2 mammary glands.
732 Wnt-1 expression was determined by qPCR, plots show means plus SEM of three
733 technical replicates; individual experiments N=3 for Raw264.7 and N=2 for MTMs.
734 Comma-1D cells were grown as monolayers (M) and Raw-264.7-mCherry macrophages
735 were added (N) and additionally treated with DKK1 (O). Co-cultures were harvested
736 after 12h and stained against E-Cadherin. E-Cadherin signal intensity in whole section
737 was quantified. Plot (P) shows mean plus SEM; each dot represents one microscopic
738 field; independent experiments N=2.

739

740 **Figure 3: Macrophage depletion during pre-malignant stages prevents early**
741 **cancer cell dissemination.** 20wk old pre-malignant MMTV-HER2 mice were treated
742 with the anti CSF1R ASF98 antibody and animals were harvested after two weeks with
743 no signs of invasive carcinoma (A). Analysis of HE staining of mammary gland sections
744 confirmed the absence of invasive lesions (B). E-Cadherin expression in whole

745 mammary glands was determined by RealTime PCR of whole mammary gland lysates
746 (**D**; mean plus SEM; each dot represents one individual mammary glands; N=2
747 experiments combined) and by immunofluorescent staining against E-Cadherin in
748 mammary gland sections (**E,F**; bars 10 μ m). E-Cadherin signal intensity was measured
749 in regions of cell junctions (**G**). Box plots depict values of individual regions for 3
750 animals each; N=2. Early circulating cancer cells (eCCCs) were quantified by harvesting
751 peripheral blood and determining the amount of HER2 and CK8/18 positive eCCs per
752 mL blood which then were normalized to the mean of controls. Plot (**H**) depicts
753 normalized means plus SEM; each dot represents one animal; combined independent
754 experiments N=2. Disseminated eCCs were quantified by staining lung sections against
755 HER2 (**I,J**; bars 25 μ M) and quantifying the average of HER2+ cells per 100 randomly
756 chosen microscopic fields (**K**). Plot (**K**) shows means + SEM where each dot represents
757 one animal of 2 individual experiments combined.

758

759 **Figure 4: Early disseminated cancer cells can contribute to metastasis formation.**

760 Macrophages were depleted from pre-malignant MMTV-HER2 mice by ASF98
761 treatment starting at week 18. Treatment was stopped when mice developed palpable
762 tumors (1-3mm average) (**A**). Mice were left until tumors reached 1cm in diameter and
763 then sacrificed. Time from beginning of treatment at age wk18 until development of
764 palpable tumors (**B**) and from formation of palpable tumors until tumors were overt (**C**)
765 is depicted as mean plus SEM where each dot represents one animal of two
766 independent experiments combined. Macrophages in sections of overt tumors at the
767 end of the experiment identified by staining against F4/80 (**D,E**) and quantified as

768 numbers of macrophages relative to tumor area (**F**). Vascularization of overt tumors was
769 analyzed by staining against endomucin, an endothelial cell marker (**G,H**) and
770 quantification of vascularized area (**I**). Plots show mean plus SEM where each dot
771 represents one section of at least 3 animals combined. Solitary DCCs in lung sections
772 and metastases defined as cell clusters bigger than 3 cells were quantified in lung
773 sections stained against HER2 (**K**). For solitary cell analysis, the average of DCCs or
774 metastases per 100 fields was counted; each dot represents one lung section (**J**). For
775 metastasis analysis, the total number of metastases per lung sections was quantified
776 and plotted (**L**). Number of mice N=6 (control) and N=4 (α CSF1R) animals combined;
777 independent experiments N=2.

778

779 **Figure 5: Phenotypic profiling of macrophages in early mammary cancer lesions.**

780 Whole mammary glands from FVB wild type mice or 14 and 22 week old pre-malignant
781 MMTV-HER2 mice were analyzed by mass cytometry. viSNE plots were generated from
782 myelo-monocytic cells (gating strategy **Fig.5 supplement 1B**) (**A**). Results from one
783 representative animal is shown; number of animals per group N=5; individual
784 experiments N=2. The three subpopulations were identified as Ly6C⁺ monocytes and
785 CD206^{hi} and CD206^{lo} macrophages based on their expression levels of Ly6C (**B**) and
786 CD206 (**C**). These three populations were then analyzed for their frequency amongst all
787 myelomonocytic cells (**D-F**) Dot plots show mean plus SEM of 5 animals per group,
788 each dot represents one animal. Heat plots for 3 individual animals per group with
789 expression levels of selected markers Ly6C (**B**), CD206 (**C**), Tie2 (**I**) and IdU
790 incorporation as a proliferation marker (**J**) were generated for CD206^{lo} and ^{-hi}

791 macrophages as identified in the viSNE plots. **G, H:** viSNE plot and quantification of
792 myelomonocytic population in overt MMTV-HER2 tumors. Mammary glands from FVB
793 wild type mice (**K**), MMTV-HER2 mice at 24wks (**L**) and overt MMTV-HER2 tumors (**M**)
794 were stained against CD206 and F4/80 and CD206 signal intensity in F4/80+
795 macrophages was quantified. Plot (N) depicts mean plus EM, each dot represents one
796 macrophages; 3 animals combined. Bars 10 μ m.

797

798 **Figure 6: HER2 upregulation leads to activation of NF κ B and CCL2**
799 **overexpression.** Phosphorylation of the p65 subunit of NF κ B was analyzed in Western
800 Blots of whole cell lysates of mammospheres from 20wk old pre-malignant MMTV-
801 HER2 mice (**A**). One representative plot of three independent experiments is shown. (**B**)
802 CCL2 expression in mammospheres derived from FVB wild type and pre-malignant
803 MMTV-HER2 mammary glands was measured by real time PCR analysis. Plot shows
804 means plus SEM where each dot represents one technical replicate; number of
805 individual experiments N=3. (**C**) Mammary glands from FVB wild type, 14wk old and
806 22wk old MMTV-HER2 mice were stained against CCL2, HER2, and CCR2. CCL2
807 immunofluorescent signal intensity around the ductal epithelium was quantified (**D**). Plot
808 shows mean plus SEM, each dot represents one duct. Bars 25 μ m. CCL2 was stained in
809 acini cultures derived from pre-malignant MMTV-HER2 mammary glands that were
810 grown for 5d and then treated with DMSO (vehicle control; **E**), 1 μ M Lapatinib (**F**) or 1 μ M
811 IKK inhibitor compound A (**G**) for 24h. Acini derived from 20 week old pre-malignant
812 MMTV-HER2 mammary glands were grown for 5d, then treated with DMSO (vehicle
813 control), Lapatinib (1 μ M), IKK inhibitor compound A (1 μ M), or CCR2 inhibitor RS504393

814 (1 μ M) and macrophages isolated from 20wk old pre-malignant MMTV-HER2 mammary
815 glands were added. After 24h, acini were stained against F4/80 and the percentage of
816 acini associated with mammary gland macrophages in 3D co-cultures (exemplary image
817 in **H**) compared to those not associated with macrophages (**I**) was determined (bar
818 25 μ m). Plot (**J**) shows means plus SEM; each dot represents one technical replicate;
819 independent experiments N=2. 20wk old pre-malignant MMTV-HER2 mice were treated
820 with a CCR2 inhibitor RS504393 (2mg/kg i.p. daily) for 2 weeks. Additionally, mice were
821 treated locally by injecting 2mg/kg CCR2 inhibitor into the fat pad of one gland and
822 vehicle control into the contra-lateral gland. Injections were performed daily for 5 days
823 (**N**). Pre-malignant mammary glands were stained against E-Cadherin and F4/80 (**K,L**,
824 bars 25 μ m) and intra-epithelial macrophage (IEM) containing ducts were quantified
825 (**M,O**). For local treatment, values were normalized to the IEM content of each contra-
826 lateral control treated gland. Plot shows means plus SEM; each dot represents one
827 animal.

828 **Figure 7: Intra-epithelial macrophage numbers in human DCIS lesions negatively**
829 **correlate with E-Cadherin levels.** Human adjacent healthy (**A**) and DCIS tissue (**B**)
830 was stained against CD68 (macrophages) and smooth muscle actin (SMA). Bar: 75 μ m.
831 Plot shows mean plus SEM of the percentage of ducts intra-epithelial macrophages
832 (IEM) from 7 healthy and 10 DCIS patients; each dot represents one patient (**C**).
833 Sections from human DCIS tissue were stained against CD68 (macrophages) and E-
834 Cadherin (**D,E**). E-Cadherin pixel intensity was quantified in regions of individual cell
835 junctions and medians for individual patients were quantified. Plot (**F**) depicts mean E-
836 Cadherin intensity throughout DCIS lesions of individual patients with low or high intra-

837 epithelial macrophage (IEM) numbers (total patient number N=12). All bars 25 μ m.
838 Scheme of macrophage (G) assisted early dissemination from pre-invasive lesions
839 where mammary tissue macrophages (MTM) are attracted into pre-invasive ducts by
840 early cancer cells (CC) via HER2 and NF κ B mediated upregulation of CCL2. Intra-
841 epithelial macrophages secrete Wnt proteins and thereby induce an EMT that drives
842 early dissemination. Early disseminated cancer cells then contribute to metastasis
843 formation, either as a slow cycling seeds of metastasis (scenario 1) or by interacting
844 with the microenvironment to make it more permissive for the growth of more adapted
845 late cancer cells (scenario 2).

846

847

848 **Supplementary Figure Legends.**

849

850 **Supplementary Fig.1.** Depletion of mammary gland macrophages (F4/80+/CD11b+) after two weeks of treatment with a CSF1R antibody compared to vehicle control (**A**). Percentage of ducts with intra-epithelial macrophages (IEM; **B**) and hyperplastic ducts (**C**) was quantified in mammary gland sections after two weeks of CSF1R antibody or vehicle treatment. Whole mount staining of mammary glands after two weeks of CSF1R antibody or vehicle control treatment (**D,E**).

856

857 **Supplementary Fig.2.** Flow cytometry lung gating strategy were CD45+ viable cells were identified as F4/80+/Gr1+/CD11b+ and F4/80-/Gr1+/CD11b+ monocytes and F4/80+/Gr1-/CD11c^{hi} alveolar macrophages (**A,B**). Quantification of alveolar macrophage (**C**) and monocyte populations (**D,E**) in lungs of MMTV-HER2 mice that had been treated with a CSF1R antibody or vehicle control during pre-malignant stages and were then allowed to progress to over tumor stages.

863

864 **Supplementary Fig.3.** **A:** List of markers analyzed by mass cytometry (CyTOF). **B:** Gating scheme to create viSNE plots of macrophages and monocytes. DNA staining and Cisplatin was used to identify viable cells. **C:** Heatplot of CD11b in the three myelomonocytic populations identified by visne plot (Fig.2A). N=3 animals per group; independent experiments: N=2. **D:** Heatplot of VCAM1 in the three myelomonocytic populations identified by viSNE plot. N=2 animals per group; independent experiments N=2.

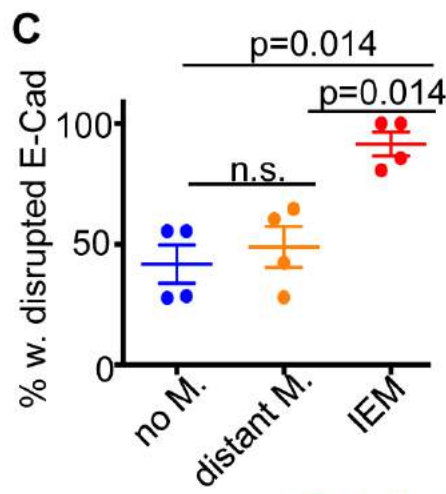
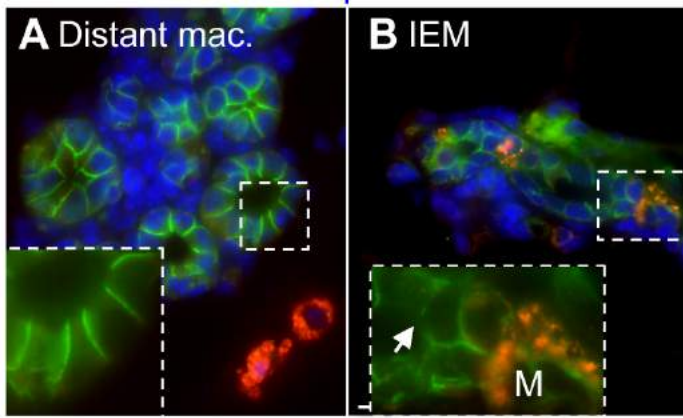
871 **Supplementary Fig.4. A:** Overview of qRT-PCR expression and immunofluorescent
872 analysis results of selected cytokines in mammospheres derived from 20wk old MMTV-
873 Her2 mammary glands that were not detectable (n.d.), did not change (n.c.) or did not
874 change significantly (n.s.) or were increased in relation to expression levels in FVB wild
875 type mammary glands. **B:** qRT-PCR expression analysis of CSF2 expression in
876 mammospheres derived from either FVB wild type or 20wk old MMTV-Her2 pre-
877 malignant mice. Three independent experiments with triplicates were performed. **C-E:**
878 Immunofluorescent staining of FVB wild type (C) and 22wk old MMTV-Her2 mammary
879 glands (D) against CSF2 or with IgG control (E). Bars 25 μ M

880

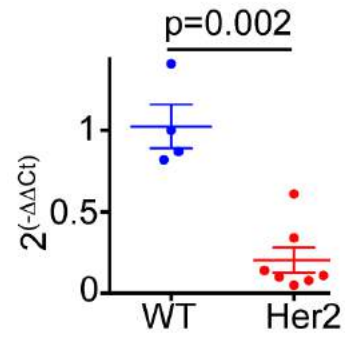
881 **Supplementary Fig.5.** Human DCIS sections were stained against CD68 and CD45 (**A**)
882 and CD68 and cytokeratin 8/18 (**B**). **B,C:** Two individual ducts in one DCIS lesion of the
883 same patient with either high E-Cadherin and low intra-epithelial macrophage (IEM)
884 levels (**C**) or low E-Cadherin levels and high IEM levels (**D**) within the same patient. **E:**
885 Quantification of E-Cadherin signal intensity in the region of cell junctions within ducts of
886 the same patients with either high or low numbers of IEMs.

887

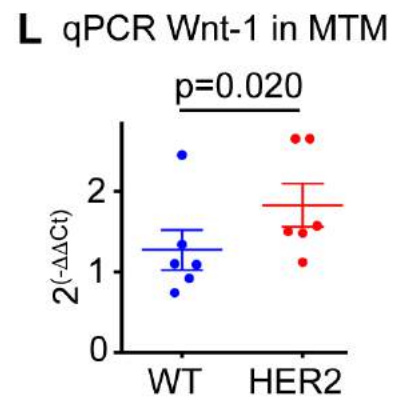
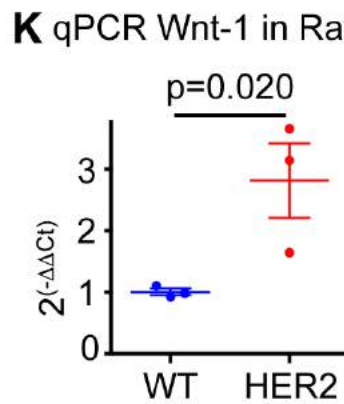
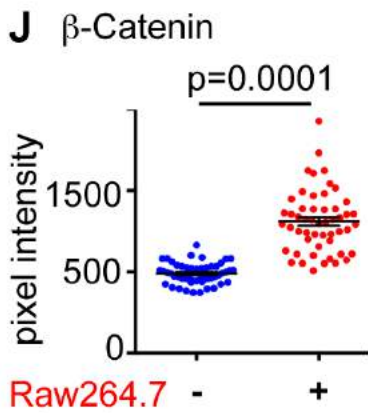
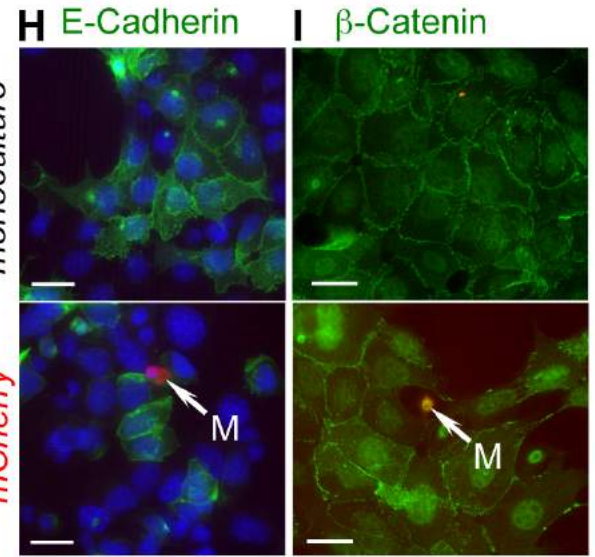
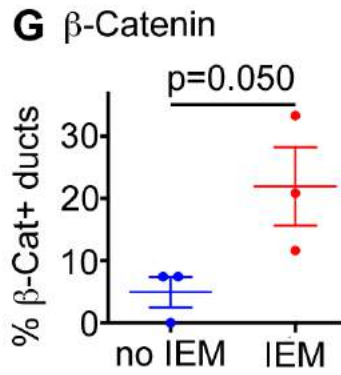
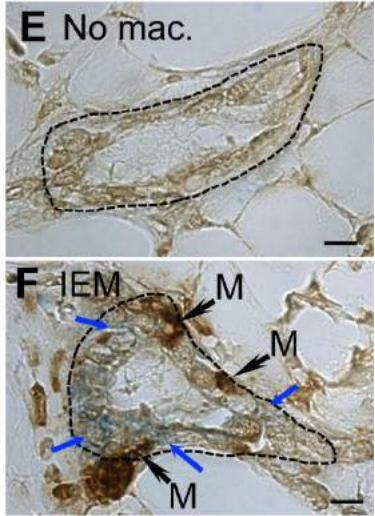
E-Cadherin F4/80 Dapi



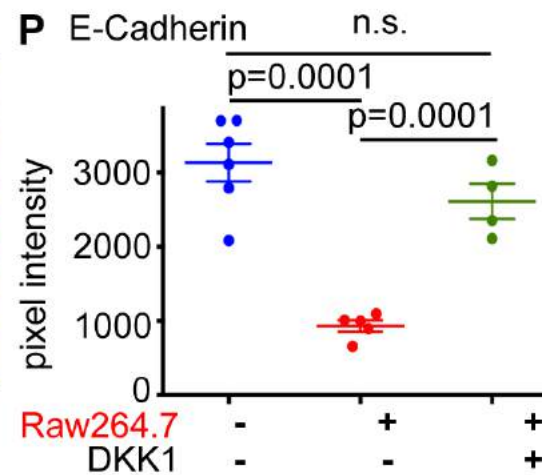
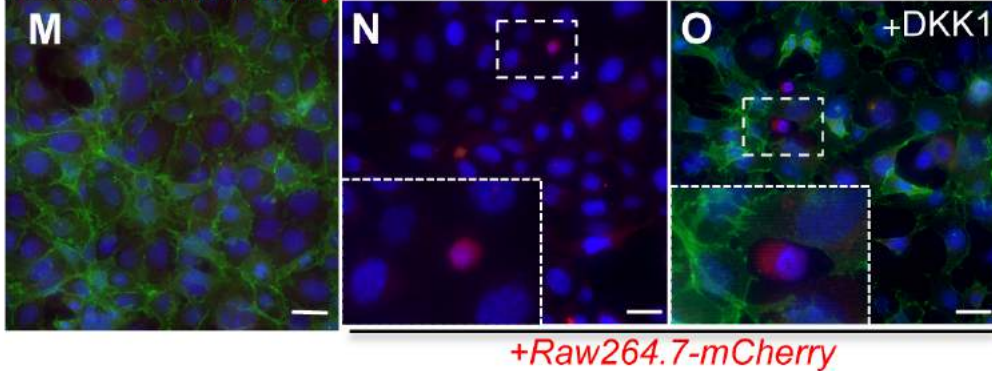
D qPCR E-Cadherin

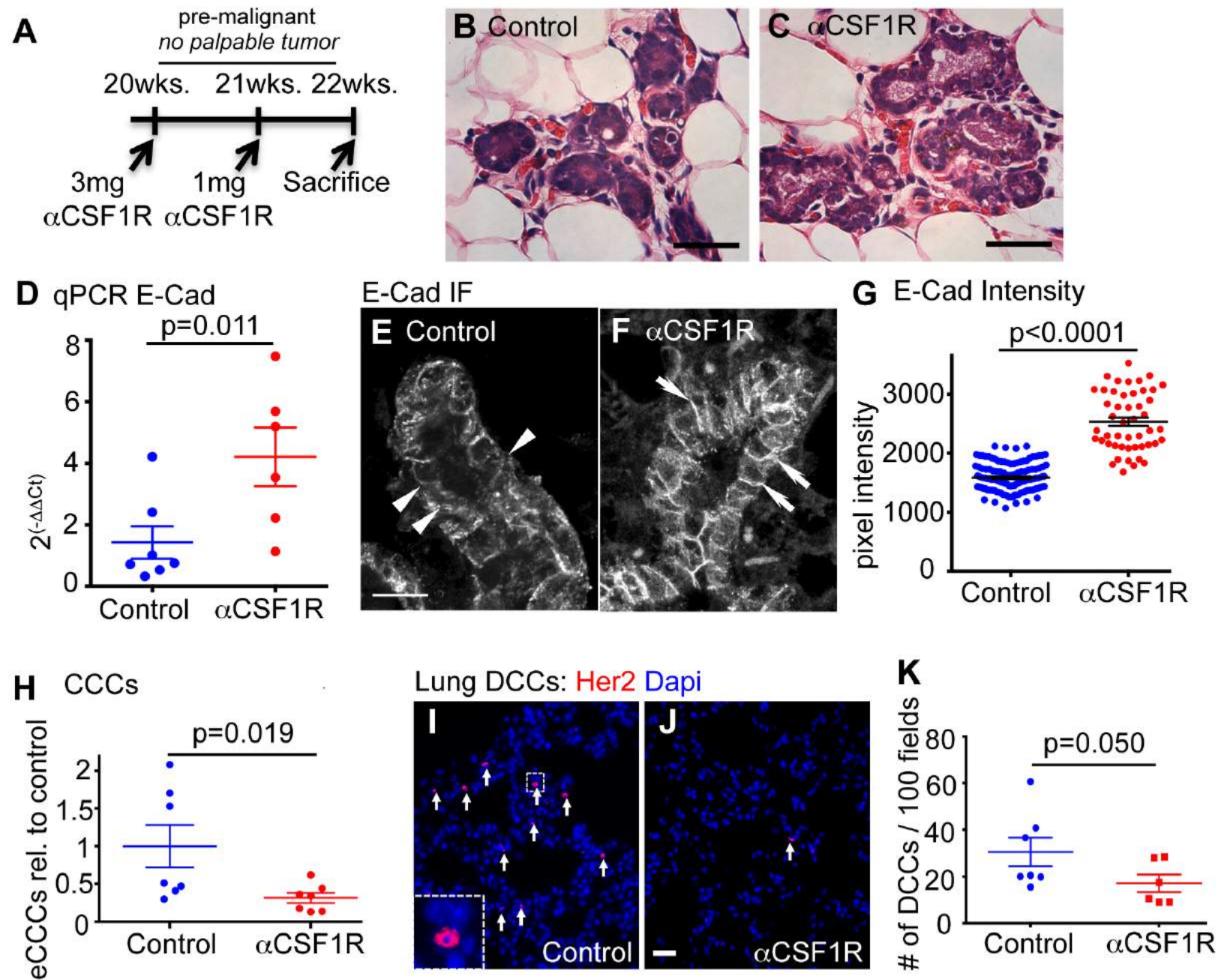


β-Catenin Iba1

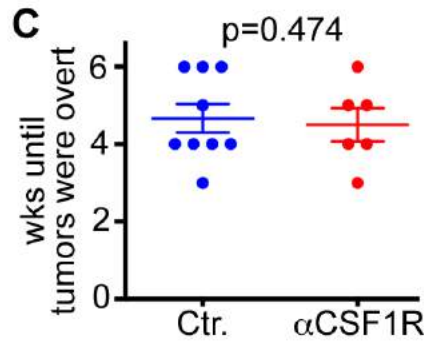
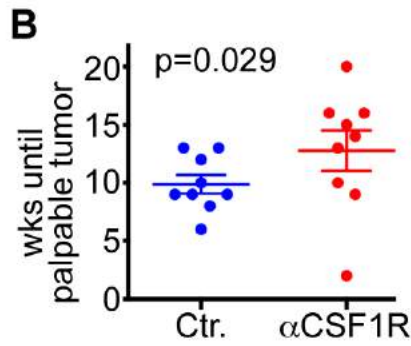
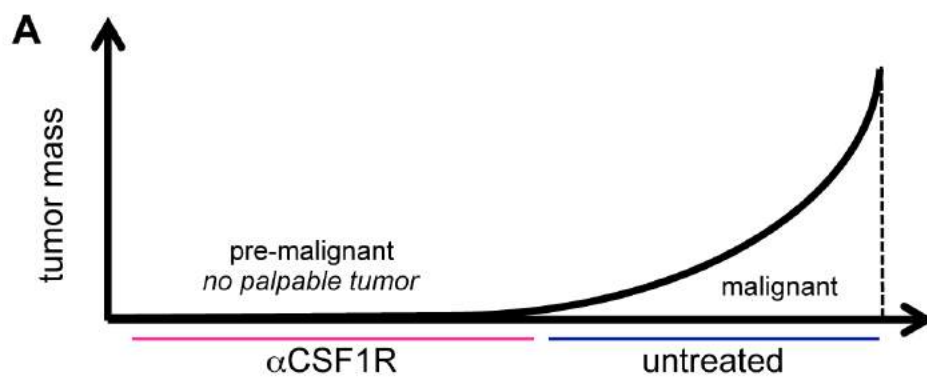


E-Cadherin mCherry

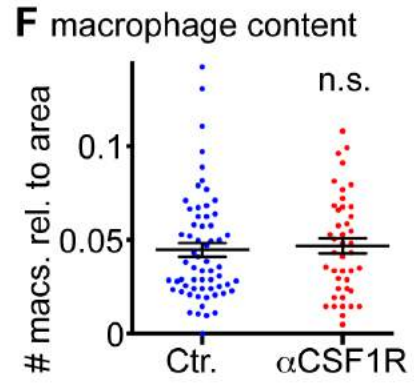
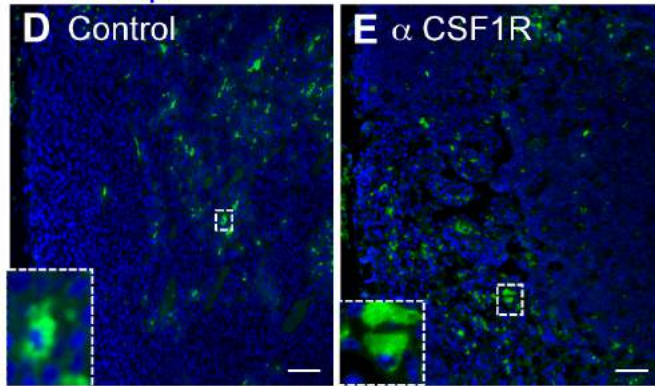




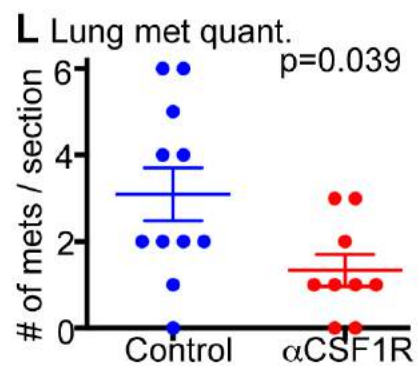
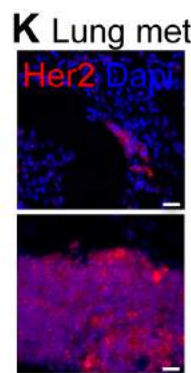
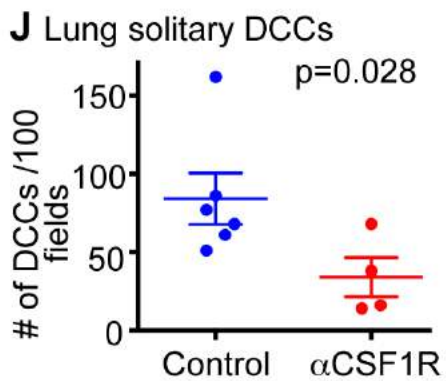
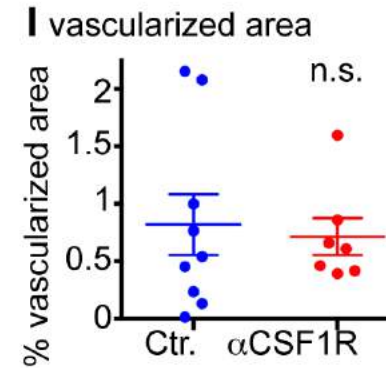
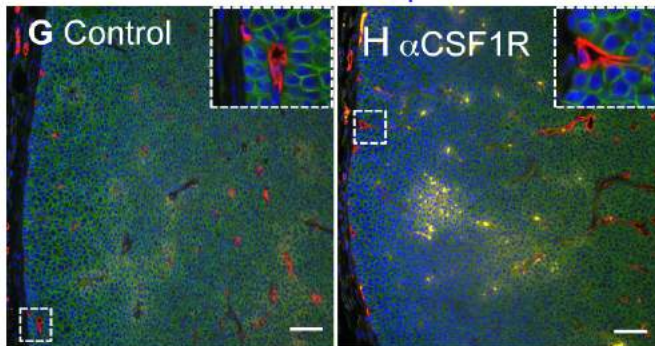
Linde et al. 2016 Figure 3



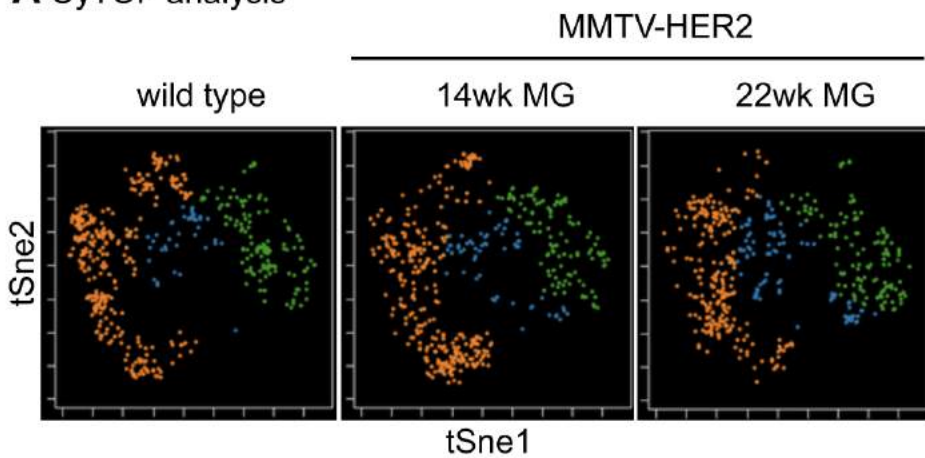
F4/80 Dapi



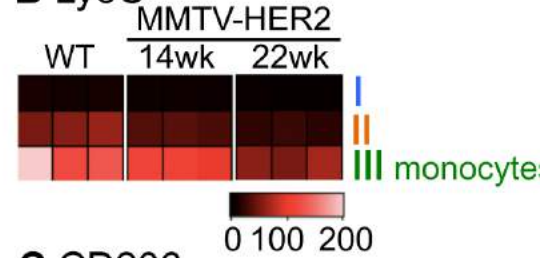
E-Cadherin Endomucin Dapi



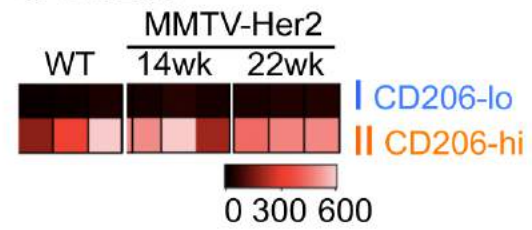
A CyTOF analysis



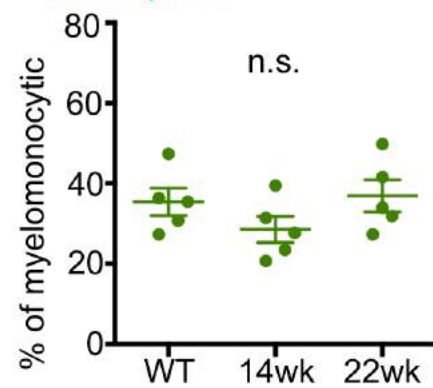
B Ly6C



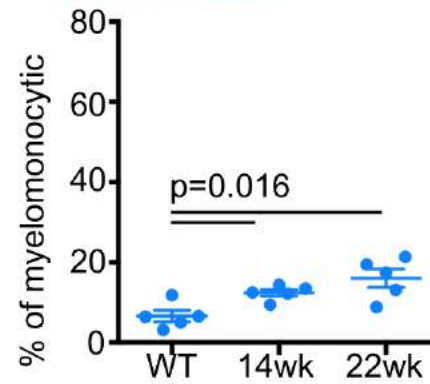
C CD206



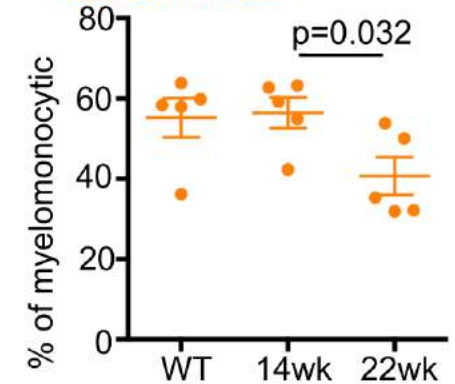
D Monocytes



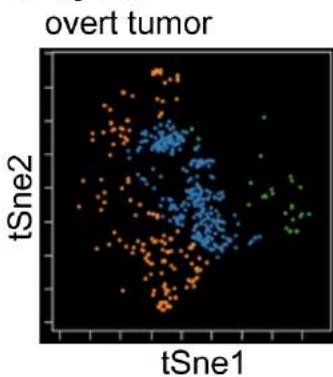
E CD206-lo Macs.



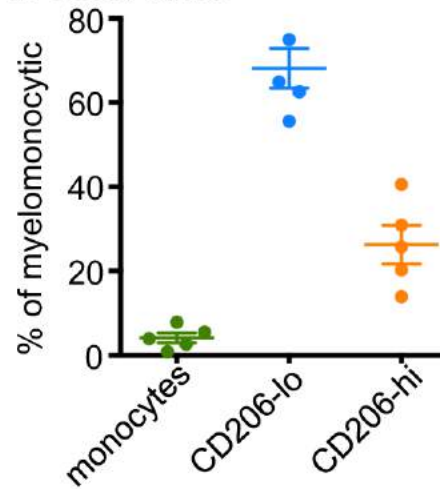
F CD206-hi Macs.



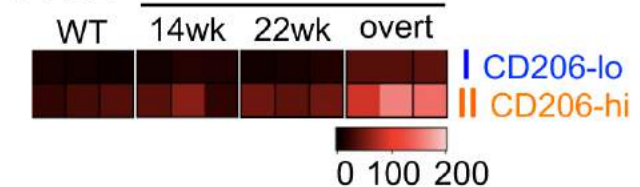
G CyTOF



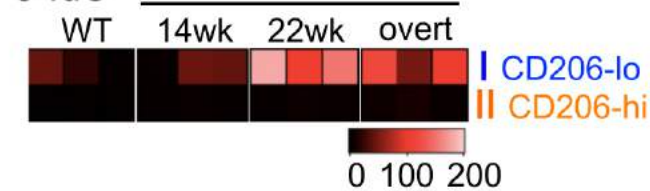
H overt tumor



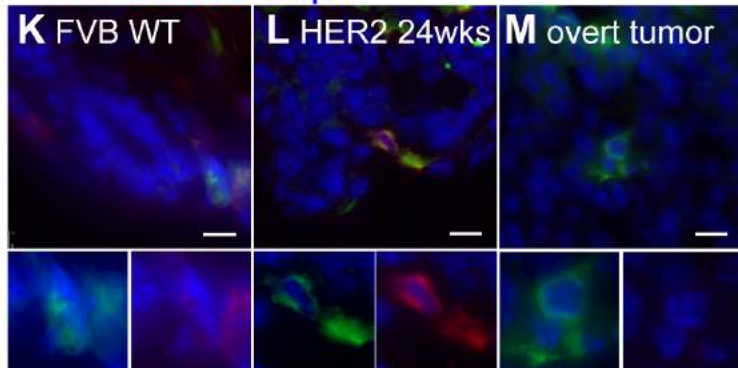
I Tie2



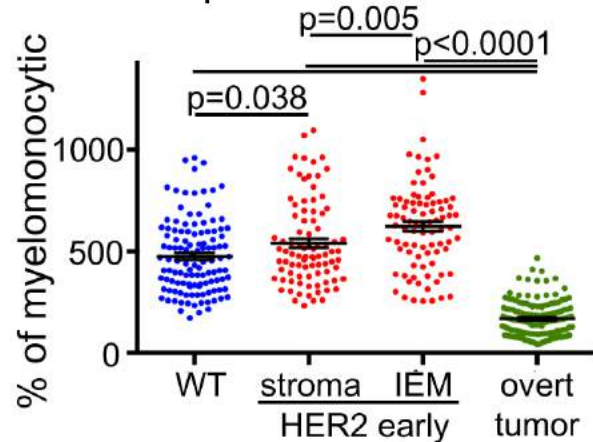
J IdU

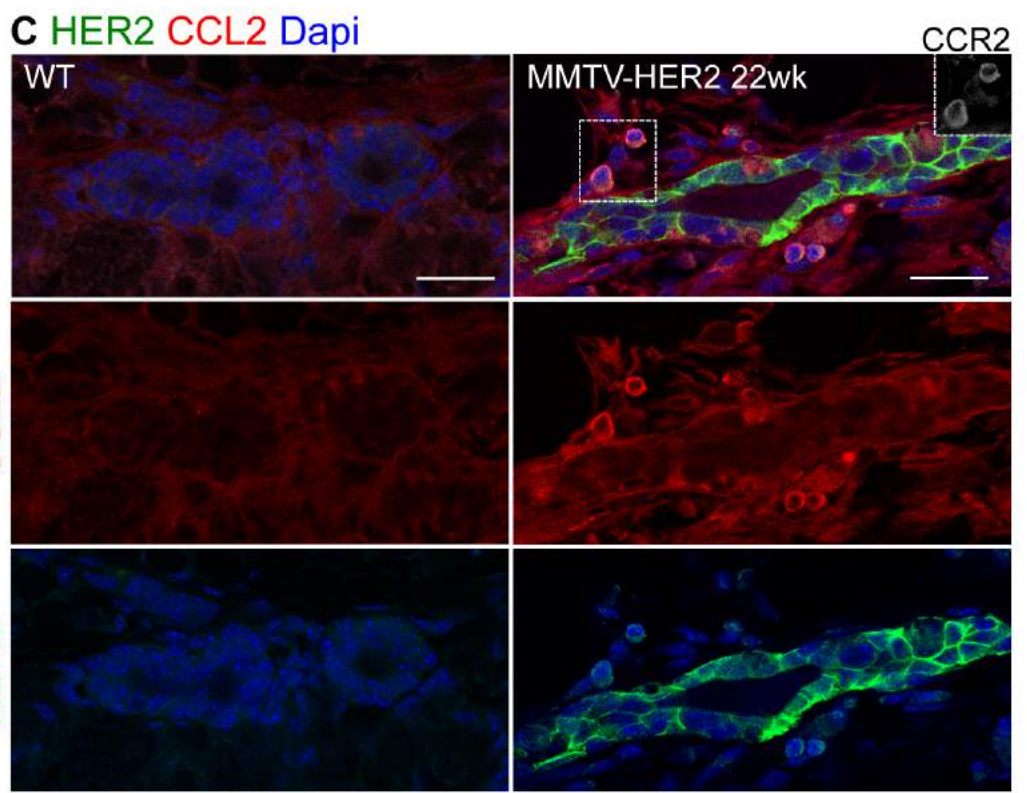
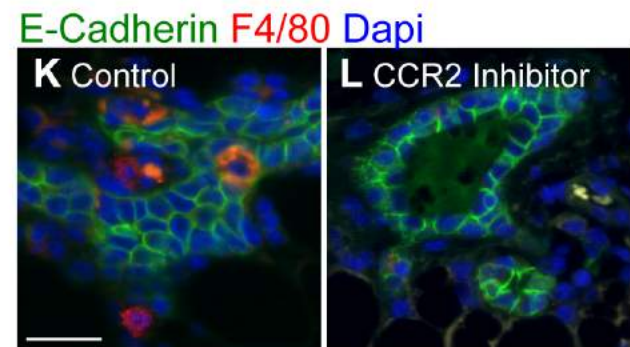
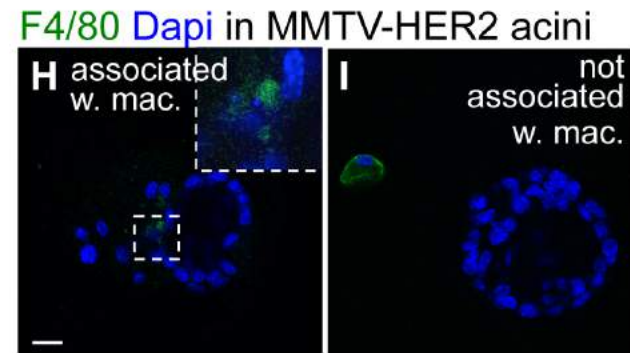
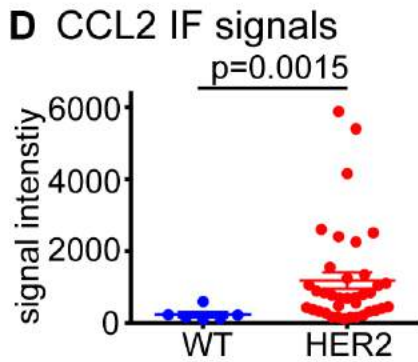
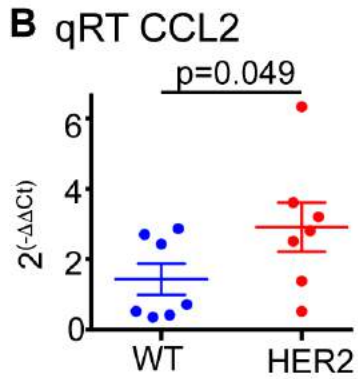
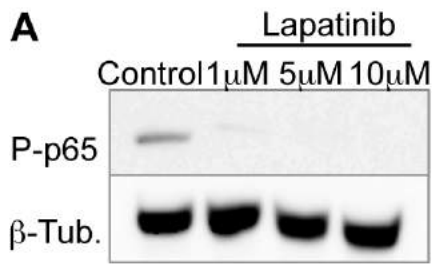


K F4/80 CD206 Dapi

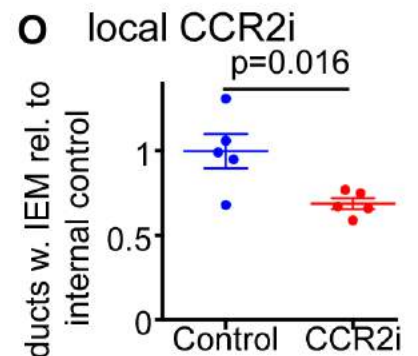
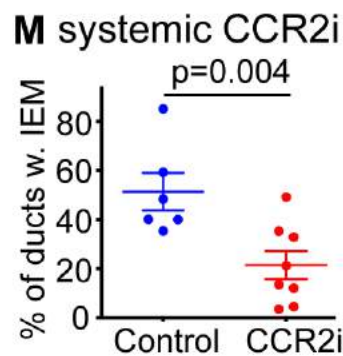
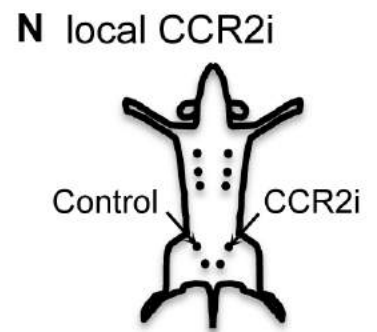
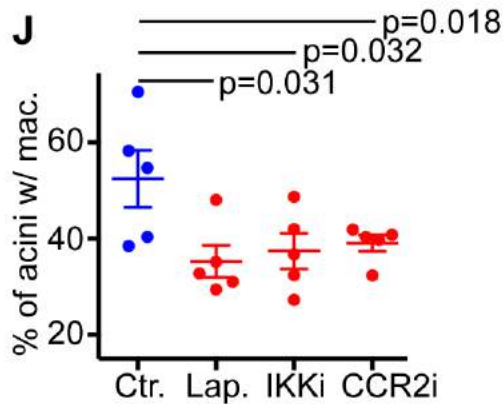
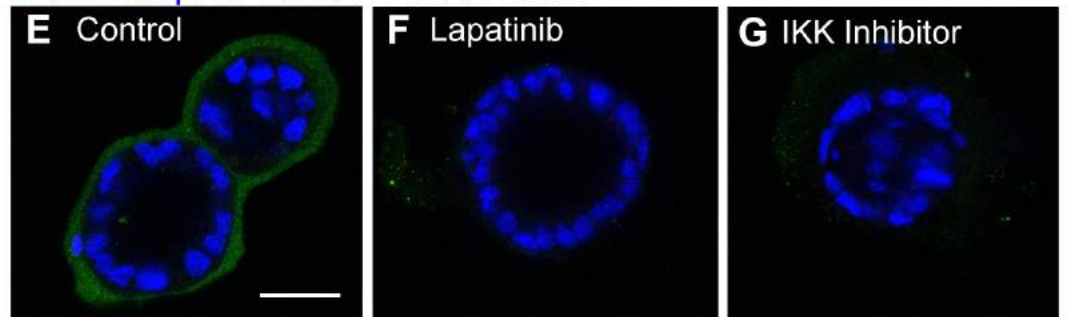


N CD206 quantification

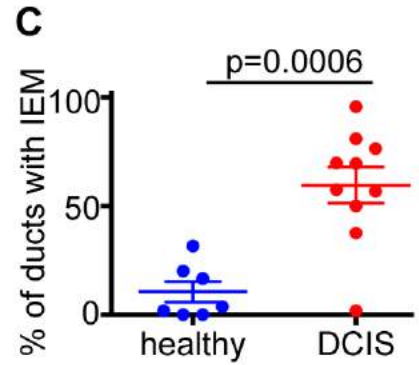
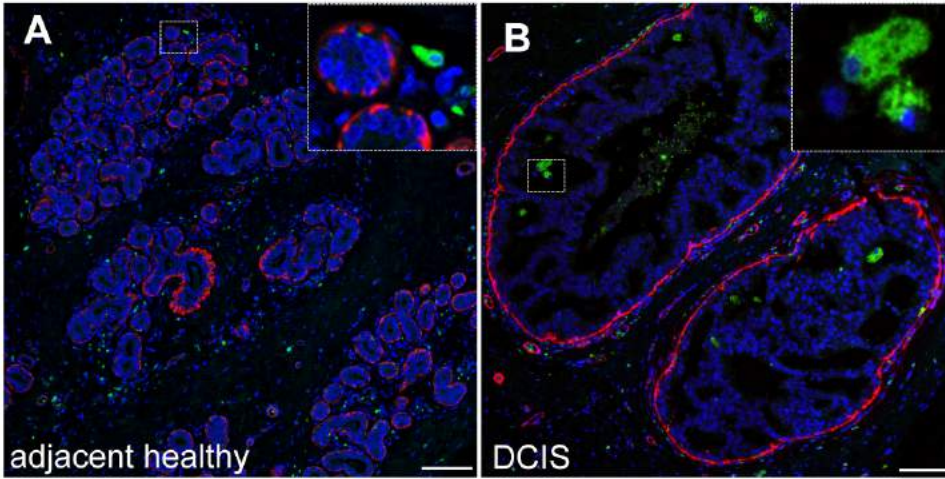




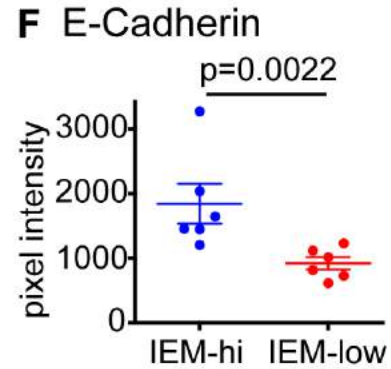
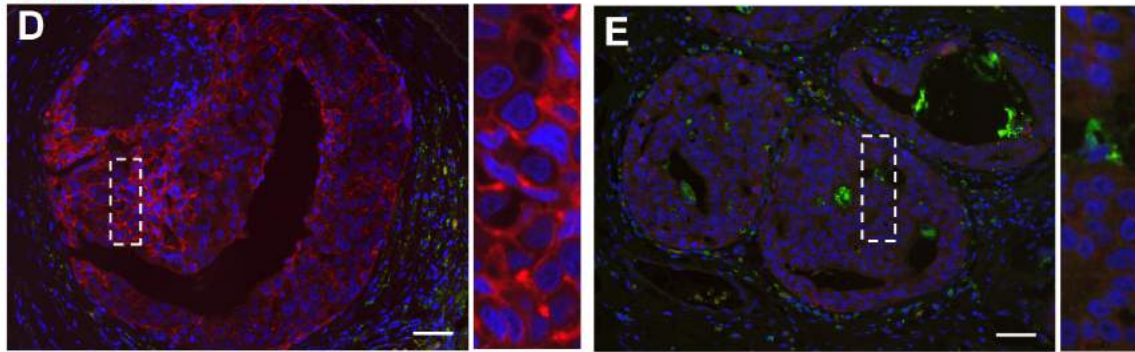
CCL2 Dapi in MMTV-HER2 acini



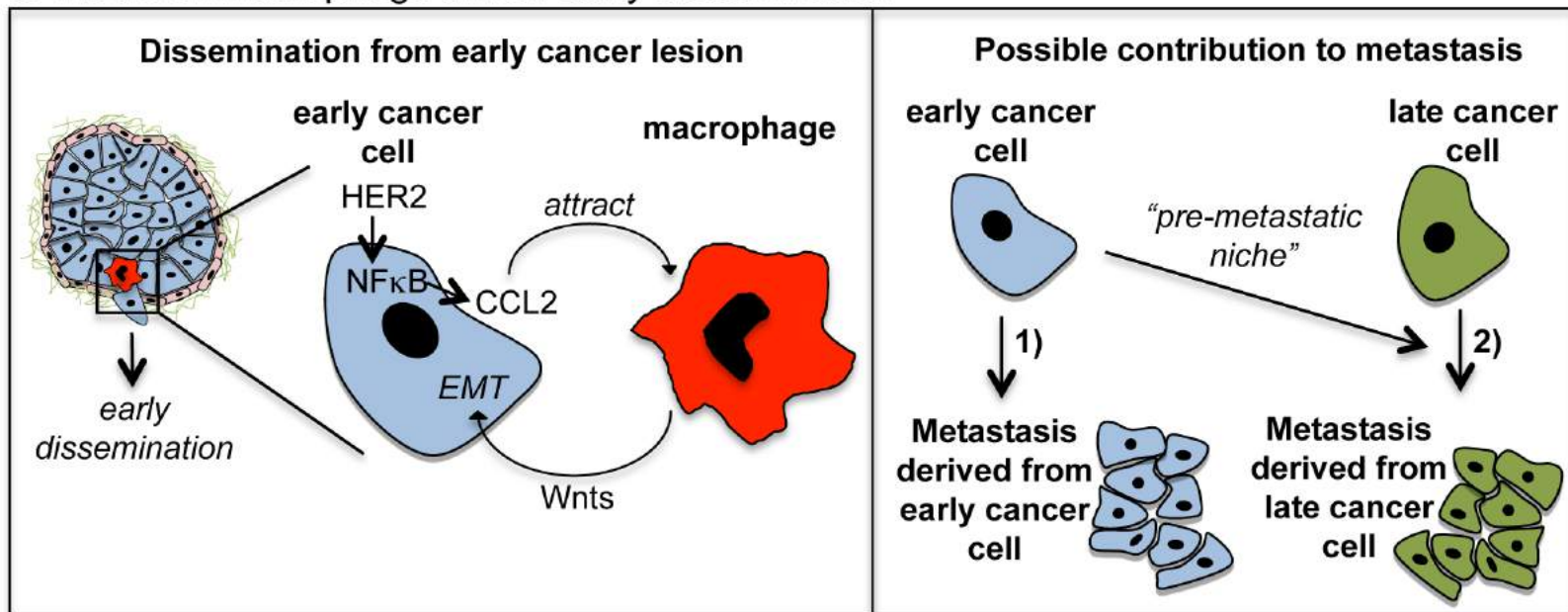
CD68 SMA DAPI



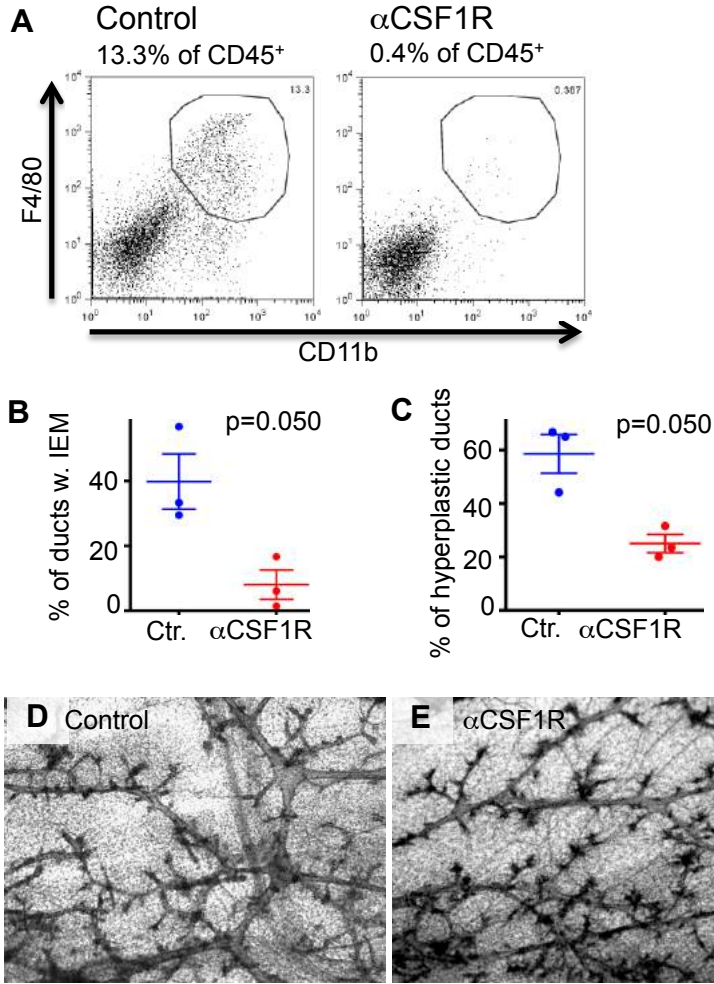
E-Cadherin CD68 DAPI



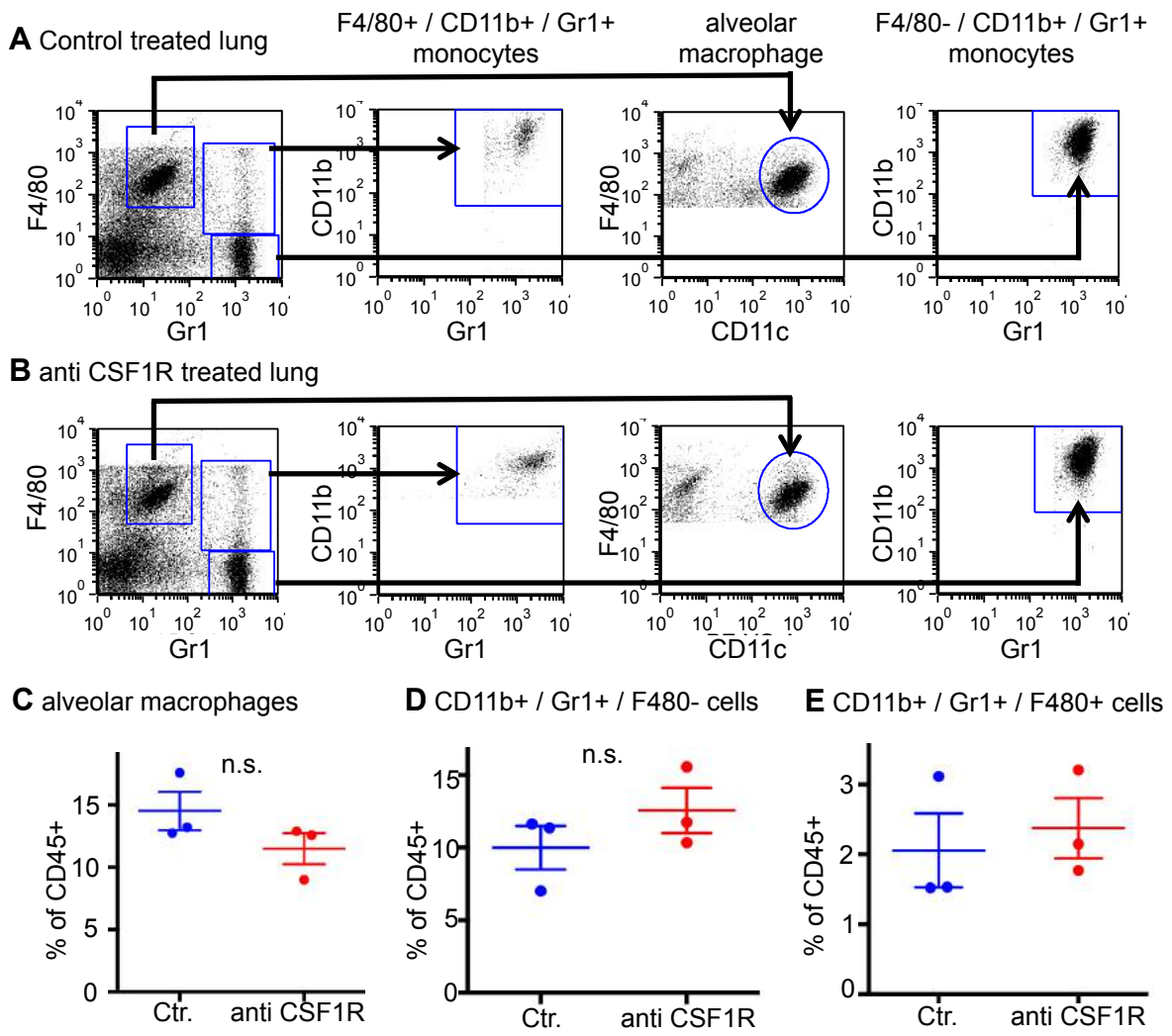
G Model of macrophage driven early dissemination



Linde et al. 2016 Figure 7



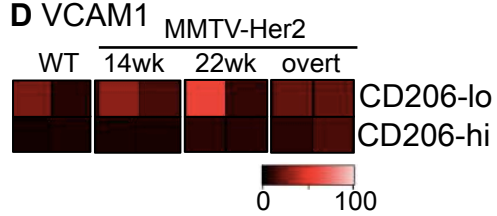
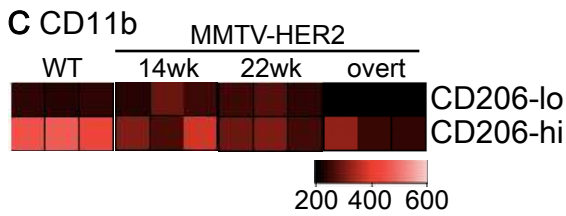
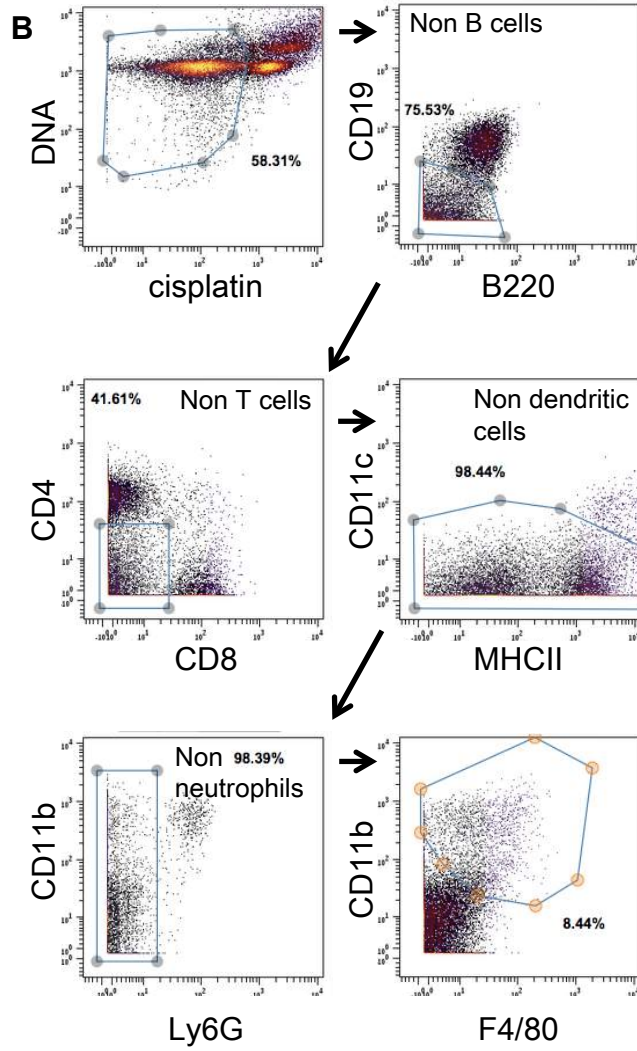
Linde et al. 2016 Supplementary Fig.1



Linde et al. 2016 Supplementary Figure 2

A

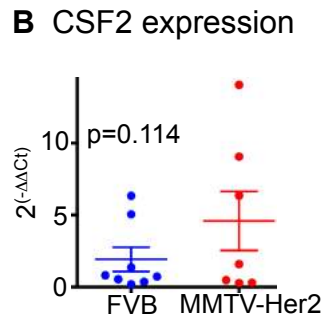
Ly6G
CD11c
CD115
CD45
CD11b
CD19
CD24
CD86
CD64
F4/80
FITC-VCAM
Ly6C
APC-CD206
CD103
cKit
CD8
Biotin-Tie2
CD4
MHCII
B220
Cisplatin
IdU



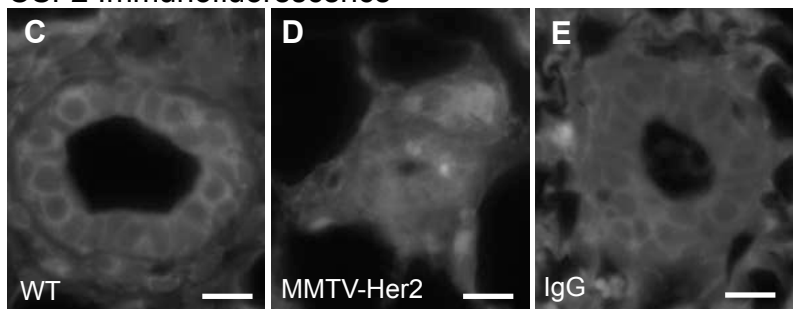
Linde et al. 2016 Supplementary Figure 3

A

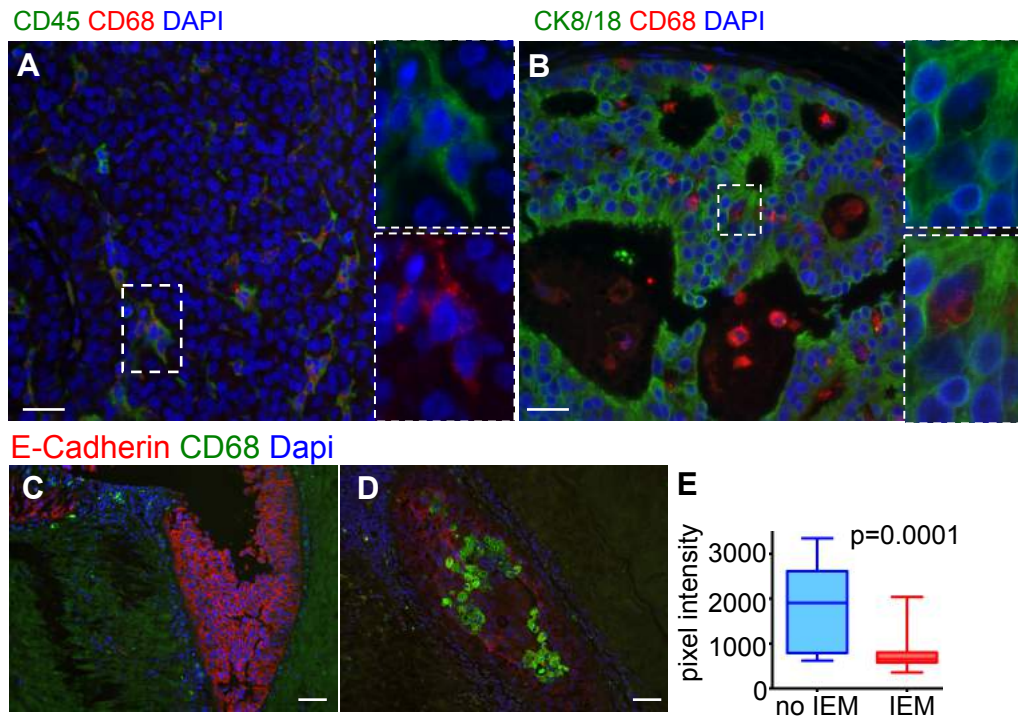
	qRT	IF
IL1b	n.d.	-
IL6	n.d.	-
CSF1	n.c.	-
CSF2	n.s.	n.c.
CCL2	increased	increased



CSF2 Immunofluorescence



Linde et al. 2016 Supplementary Figure 4



Linde et al. 2016 Supplementary Figure 5